NASA TECHNICAL MEMORANDUM

NASA TM X-3530

NASA TM X-3530

SUBSONIC AND SUPERSONIC AERODYNAMIC CHARACTERISTICS OF A SUPERSONIC CRUISE FIGHTER MODEL WITH A TWISTED AND CAMBERED WING WITH 74° SWEEP

Odell A. Morris

Langley Research Center
Hampton, Va. 23665

NATIONAL AERONAUTICS AND SPACE ADMINISTRATION • WASHINGTON D. C. • AUGUST 1977

1. Report No.	2. Government Accession No.	3. Recipient's Catalog No.
NASA TM X-3530		

4. Title and Subtitle
SUBSONIC AND SUPERSONIC AERODYNAMIC CHARACTERISTICS OF A SUPERSONIC CRUISE FIGHTER MODEL WITH A TWISTED AND CAMBERED WING WITH 74° SWEEP

5. Report Date
August 1977

6. Performing Organization Code

7. Author(s)
Odell A. Morris

8. Performing Organization Report No.
L-11457

10. Work Unit No.
505-11-21-03

9. Performing Organization Name and Address
NASA Langley Research Center
Hampton, VA 23665

11. Contract or Grant No.

13. Type of Report and Period Covered
Technical Memorandum

12. Sponsoring Agency Name and Address
National Aeronautics and Space Administration
Washington, DC 20546

14. Sponsoring Agency Code

15. Supplementary Notes

16. Abstract
A wind-tunnel investigation has been conducted in the Mach number range from 0.60 to 2.96 at a Reynolds number of 6.56×10^6 per meter to determine the longitudinal and lateral aerodynamic characteristics of a model of a supersonic cruise fighter configuration with a design Mach number of 2.60. The configuration is characterized by a highly swept arrow wing twisted and cambered to minimize supersonic drag due to lift, twin wing-mounted vertical tails, and an aft-mounted integral underslung duel-engine pod. The investigation also included tests of the configuration with larger outboard vertical tails and with small nose strakes.

Results of the investigation showed that the maximum values of lift-drag ratio for the complete basic configuration varied from about 7.5 at subsonic speeds to about 6.3 at the design Mach number of 2.60. The complete configuration had sufficient positive zero-lift pitching moment so that for conditions of neutral subsonic stability, trimmed supersonic cruise flight could be maintained with little or no trim drag. Only the configuration with the large vertical and ventral tails indicated positive levels of directional stability for lift coefficients up to 0.1 at a Mach number of 2.60. The addition of nose strakes to the model also provided small improvements in directional stability at the higher lift coefficients.

17. Key Words (Suggested by Author(s))	18. Distribution Statement
Wind-tunnel tests Lateral aerodynamic characteristics Longitudinal aerodynamic characteristics Supersonic cruise fighter configuration	Unclassified - Unlimited Subject Category 02

19. Security Classif. (of this report)	20. Security Classif. (of this page)	21. No. of Pages	22. Price*
Unclassified	Unclassified	61	$4.50

*For sale by the National Technical Information Service, Springfield, Virginia 22161

SUBSONIC AND SUPERSONIC AERODYNAMIC CHARACTERISTICS OF A SUPERSONIC CRUISE FIGHTER MODEL WITH A TWISTED AND CAMBERED WING WITH 74° SWEEP

Odell A. Morris
Langley Research Center

SUMMARY

A wind-tunnel investigation has been conducted in the Mach number range from 0.60 to 2.96 at a Reynolds number of 6.56×10^6 per meter to determine the longitudinal and lateral aerodynamic characteristics of a model of a supersonic cruise fighter configuration with a design Mach number of 2.60. The configuration is characterized by a highly swept arrow wing twisted and cambered to minimize supersonic drag due to lift, twin wing-mounted vertical tails, and an aft-mounted integral underslung dual-engine pod. The investigation also included tests of the configuration with larger outboard vertical tails and with small nose strakes.

Results of the investigation showed that the maximum values of lift-drag ratio for the complete basic configuration varied from about 7.5 at subsonic speeds to about 6.3 at the design Mach number of 2.60. The complete configuration had sufficient positive zero-lift pitching moment so that for conditions of neutral subsonic stability, trimmed supersonic cruise flight could be maintained with little or no trim drag. Only the configuration with the large vertical and ventral tails indicated positive levels of directional stability for lift coefficients up to 0.1 at a Mach number of 2.60. The addition of nose strakes to the model also provided small improvements in directional stability at the higher lift coefficients.

INTRODUCTION

As a result of current U.S. Air Force interest in supersonic cruise (Supercruiser) fighter aircraft, the National Aeronautics and Space Administration has undertaken a research program to advance the aerodynamic technology underlying the design of such vehicles. Beyond building an appropriate aerodynamic data base, specific purposes of the program are to assess the applicability of current "slender-body" design methods to such low-fineness-ratio configurations and to define promising configuration concepts over a range of supersonic Mach numbers. Initial analytical and experimental results of the effort have been presented in references 1 and 2.

This paper presents the results of tests of that configuration having the highest design cruise Mach number (2.60) of the series. The configuration is

characterized by a highly swept and warped arrow wing, twin wing-mounted vertical tails, and an integral aft-mounted underslung dual-engine pod.

Wind-tunnel tests of the basic configuration were conducted in the Langley 8-foot transonic pressure tunnel and in the Langley Unitary Plan wind tunnel over a range of Mach numbers from 0.60 to 2.96 and at a Reynolds number of 6.56×10^6 per meter. Tests over a limited supersonic range were made of the configuration with small nose strakes and with larger vertical and ventral tails. Results are presented with limited analysis.

SYMBOLS

The data in the present investigation are referenced to the body-axis system except for the lift and drag coefficients which are referenced to the stability-axis system. The moment reference center is located on the body axis 84.51 cm rearward of the nose of the model at a longitudinal station corresponding to 73 percent of the body length. Values are given in SI units.

b	reference wing span, 60.040 cm
C_D	drag coefficient, Drag/qS
$C_{D,0}$	drag coefficient at zero lift
C_L	lift coefficient, Lift/qS
C_l	rolling-moment coefficient
C_{l_β}	effective dihedral parameter, $\partial C_l/\partial\beta$ at $\beta = 0^\circ$
C_m	pitching-moment coefficient, Pitching moment/$qS\bar{c}$
$C_{m,0}$	pitching-moment coefficient at zero lift
$\partial C_m/\partial C_L$	longitudinal stability parameter (or static margin, percent $\bar{c}$)
C_n	yawing-moment coefficient, Yawing moment/qSb
C_{n_β}	directional stability parameter, $\partial C_n/\partial\beta$ at $\beta = 0^\circ$
C_Y	side-force coefficient, Side force/qS
C_{Y_β}	side-force parameter, $\partial C_Y/\partial\beta$ at $\beta = 0^\circ$
$\bar{c}$	mean aerodynamic chord of reference wing, 46.640 cm
L/D	lift-drag ratio
l	fuselage length
M	free-stream Mach number

q free-stream dynamic pressure, Pa

S reference wing area including fuselage intercept and outboard wingtips, 0.210 m^2

x distance from nose measured along body axis

α angle of attack, deg

β angle of sideslip, deg

Subscript:

max maximum

Model component designations:

S nose strakes

V_1 small vertical tails and small ventral fins

V_2 large vertical tails and small ventral fins

V_3 large vertical tails and large ventral fins

WB combination of wing, body, and engine pod without vertical or ventral tails

DESCRIPTION OF MODEL

The dimensional details of the wind-tunnel model are shown in figure 1. Figure 2 shows the cross-sectional development of the fuselage and propulsion pod. A photograph of the model in the Langley Unitary Plan wind tunnel is shown in figure 3. Additional geometric characteristics are listed in table I.

As noted previously, the present configuration represents the upper end in cruise speed of the series of configurations being investigated in the supercruiser technology program. The present concept involves primarily a high-speed, high-altitude cruise vehicle; little consideration is given to maneuverability. Thus, the concept has much in common with the supersonic commercial transport (SST). In fact, not only does the concept borrow heavily from the SST aerodynamic technology, but the wind-tunnel model itself is a rework of the very high performance SST wind-tunnel model (designated SCAT 15F) of reference 3. As indicated in figure 1(a), the model of the present tests was constructed by molding the fighter fuselage over the basic SCAT 15F wing-body-fin model and by integrating the dual-engine pod. Although this model construction scheme had the advantage of speed, the construction did impose physical constraints which limited the extent to which optimization could have been achieved. A camber and twist distribution which might have resulted in a slightly better drag due to lift and in improved self-trimming properties (obviating near neutral stability

at subsonic speeds to achieve trim drag-free cruise) is just such a design feature precluded by the process.

Additional components of the wind-tunnel model are shown in figure 1(b) and figure 1(c). These components are the enlarged vertical tail, the ventral fin, and the fuselage nose strakes, each of which was designed to improve the directional stability which was expected to be degraded from that of the original wing-body-fin model when the forward fuselage with the large side area was added.

TESTS AND CORRECTIONS

Static longitudinal and lateral aerodynamic characteristics of the model were measured in the Langley 8-foot transonic pressure tunnel and in the Langley Unitary Plan wind tunnel. Tests were made through an angle-of-attack range of about -6° to 9° at angles of sideslip of 0° and 2°. The dewpoint was maintained sufficiently low to prevent measurable condensation effects in the test section. Other test conditions for both tunnels are summarized in the following table:

Mach number	Stagnation pressure, kPa	Stagnation temperature, K	Reynolds number per meter
0.60	63.54	322	6.56×10^6
.80	53.86	322	6.56
.90	51.13	322	6.56
.95	49.94	322	6.56
.97	49.80	322	6.56
1.80	58.46	339	6.56
2.00	63.54	339	6.56
2.30	73.35	339	6.56
2.60	85.70	339	6.56
2.96	103.85	339	6.56

The angles of attack and sideslip were corrected for the deflection of the balance and sting under aerodynamic load and for tunnel flow angularity. The balance-chamber pressure and the base pressure were measured, and the drag force was adjusted until the base pressure equaled free-stream static pressure. In addition, the drag results have been corrected for the internal skin friction drag of the engine pod.

To assure a turbulent boundary-layer condition in the supersonic Mach number range, 0.16-cm-wide transition strips of No. 60 carborundum grit were applied 1.02 cm from the nose of the body and 1.02 cm (measured streamwise) from the leading edges of the wing and vertical tails. Transition strips were also located 1.02 cm from the inlets on both the outer and inner surfaces of the engine pod with No. 60 carborundum grit on the outer surface and No. 80 carborundum grit on the inner surface. For tests in the subsonic Mach number range ($M = 0.60$ to 0.97), strips of No. 80 carborundum grit were used instead of the larger grit used at higher Mach numbers.

PRESENTATION OF RESULTS

The results of the investigation are presented in the figures as outlined here.

DISCUSSION

Longitudinal Aerodynamic Characteristics

Figure 4 presents the longitudinal aerodynamic characteristics of the complete basic model configuration with and without the small vertical and ventral tails. The configuration exhibits reasonably linear pitching-moment characteristics at all Mach numbers except in the higher lift coefficient range. At the higher lift coefficients (above $C_L \approx 0.20$), the pitching-moment curves showed a slight tendency toward pitch-up which was somewhat more pronounced in the subsonic speed range. This behavior is presumably associated with flow separation in the region of the wingtips since the addition of the outboard vertical tails to the wing body shows a decrease in the pitch-up tendency.

The effects on longitudinal aerodynamic characteristics of increased vertical and ventral tail size and of fuselage nose strakes are shown in figures 5 and 6, respectively. Slightly increased drags where tail size is increased and an increased pitch-up tendency at the highest lift coefficients for the straked configuration are the discernible longitudinal effects.

A summary plot of the longitudinal aerodynamic parameters is shown in figure 7 for the basic model and for the model with the large tails. The data show that the maximum values of the lift-drag ratio for the basic configuration varied from about 7.5 at subsonic speeds to about 6.3 at the design Mach number of 2.60. It should be noted, however, that the tests of the model in the subsonic range were very limited and made no attempt to obtain higher L/D values through the use of variable leading- and trailing-edge flaps which have previously been demonstrated to be very effective for SST configurations in this speed range (ref. 4).

Static longitudinal stability $\partial C_m/\partial C_L$ is seen to be essentially constant throughout the measured supersonic speed range at essentially the same value (-0.10) as for Mach number 0.95. From Mach number 0.95 down to Mach number 0.60, a sharper change to a value of -0.055 is shown. In the transonic speed range where present data are sparse, data from the more extensive tests of the SCAT 15F configuration (ref. 4) reveal an increase in stability to a peak value some 3.5-percent $\bar{c}$ beyond the supersonic and Mach number 0.95 values. It should be noted that the $C_{m,0}$ values shown in this summary figure tend to peak in the same speed range as the longitudinal stability. This peak shows a compensatory effect which could minimize or eliminate trim drag across the entire speed range. In fact, in the subsonic range, slightly positive control deflection which has been shown to improve lift-drag ratio would be required for trim.

Lateral Aerodynamic Characteristics

Figures 8, 9, and 10 show the static lateral aerodynamic characteristics of the basic model, with and without the small vertical and ventral tails, with larger vertical and ventral tails, and with fuselage nose strakes, respectively. Figure 11 summarizes the static directional aerodynamic characteristics from these data, portraying C_{n_β} as a function of Mach number at lift coefficients of 0.0, 0.1, and 0.2.

The addition of the small vertical and ventral tails produced a stabilizing increment in C_{n_β} which was insufficient to provide positive directional stability in any practical operating range. The increased relative instability of the present configuration when compared with the progenitor SST configuration is attributable primarily to the increased forward-fuselage side area. The addition of the larger vertical and ventral surfaces is seen to provide large stabilizing increments in C_{n_β} as might be expected with the increase in tail area. Fuselage forebody strakes produced little if any change in C_{n_β} in the limited Mach number range over which strakes were tested until relatively high lift coefficients were reached. Within the range of the tests, no combination of components provides positive static directional stability beyond a lift coefficient of 0.1 (near design cruise) at speeds equal to or greater than the design Mach number of 2.60.

SUMMARY OF RESULTS

A wind-tunnel investigation has been conducted in the Mach number range from 0.60 to 2.96 at a Reynolds number of 6.56×10^6 per meter to determine the longitudinal and lateral aerodynamic characteristics of a model of a supersonic cruise fighter configuration with a design Mach number of 2.60. The configuration is characterized by a highly swept arrow wing twisted and cambered to minimize supersonic drag due to lift, twin wing-mounted vertical tails, and an aft-mounted integral underslung dual-engine pod. The investigation also included tests of the configuration with larger outboard vertical tails and with small nose strakes. The following results were indicated:

1. The maximum values of lift-drag ratio for the complete basic configuration varied from about 7.5 at subsonic speeds to about 6.3 at the design Mach number of 2.60.

2. The complete configuration had sufficient positive zero-lift pitching moment so that for conditions of neutral subsonic stability, trimmed supersonic cruise flight could be maintained with little or no trim drag.

3. Directional stability showed the expected improvements with increased vertical and ventral tail area and an improvement with the addition of fuselage nose strakes at the higher lift coefficients. At and above the cruise Mach number of 2.60, however, static directional stability was not demonstrated above a lift coefficient of 0.1.

Langley Research Center
National Aeronautics and Space Administration
Hampton, VA 23665
May 19, 1977

REFERENCES

1. Shrout, Barrett L.; Morris, Odell A.; Robins, A. Warner; and Dollyhigh, Samuel M.: Review of NASA Supercruise Configuration Studies. Design Conference Proceedings - Technology for Supersonic Cruise Military Aircraft, Volume I, AFFDL TR-77-85, U.S. Air Force, 1976.

2. Dollyhigh, Samuel M.; Ayers, Theodore G.; Morris, Odell A.; and Miller, David M.: Designing for Supercruise and Maneuver. Design Conference Proceedings - Technology for Supersonic Cruise Military Aircraft, Volume I, AFFDL TR-77-85, U.S. Air Force, 1976.

3. Morris, Odell A.; and Fournier, Roger H.: Aerodynamic Characteristics at Mach Numbers 2.30, 2.60, and 2.96 of a Supersonic Transport Model Having a Fixed, Warped Wing. NASA TM X-1115, 1965.

4. Morris, Odell A.; and Patterson, James C., Jr.: Transonic Aerodynamic Characteristics of Supersonic Transport Model With a Fixed, Warped Wing Having 74° Sweep. NASA TM X-1167, 1965.

TABLE I.- GEOMETRIC CHARACTERISTICS OF MODEL

Wing:	
Aspect ratio	1.717
Span, cm	60.046
Area, m^2	0.21
Root chord at fuselage center line, cm	71.790
Tip chord, cm	3.574
Mean aerodynamic chord, cm	46.650
Thickness-chord ratio, root	0.032
Thickness-chord ratio, tip	0.027
Fuselage:	
Length, cm	116.20
Vertical tails:	
Small vertical area (each), m^2	0.0072
Small ventral area (each), m^2	0.0045
Large vertical area (each), m^2	0.0117
Large ventral area (each), m^2	0.0078
Airfoil section	Half-circular arc
Engine pod:	
Length, cm	49.530
Capture area, m^2	0.035
Duct internal wetted area, m^2	0.133
Inlet internal half-angle, deg	3.150
Inlet external half-angle, deg	22.890
Model volume:	
Fuselage volume, m^3	0.00406
Wing-fuselage volume (total), m^3	0.00571
$V^{2/3}/S$	0.1521

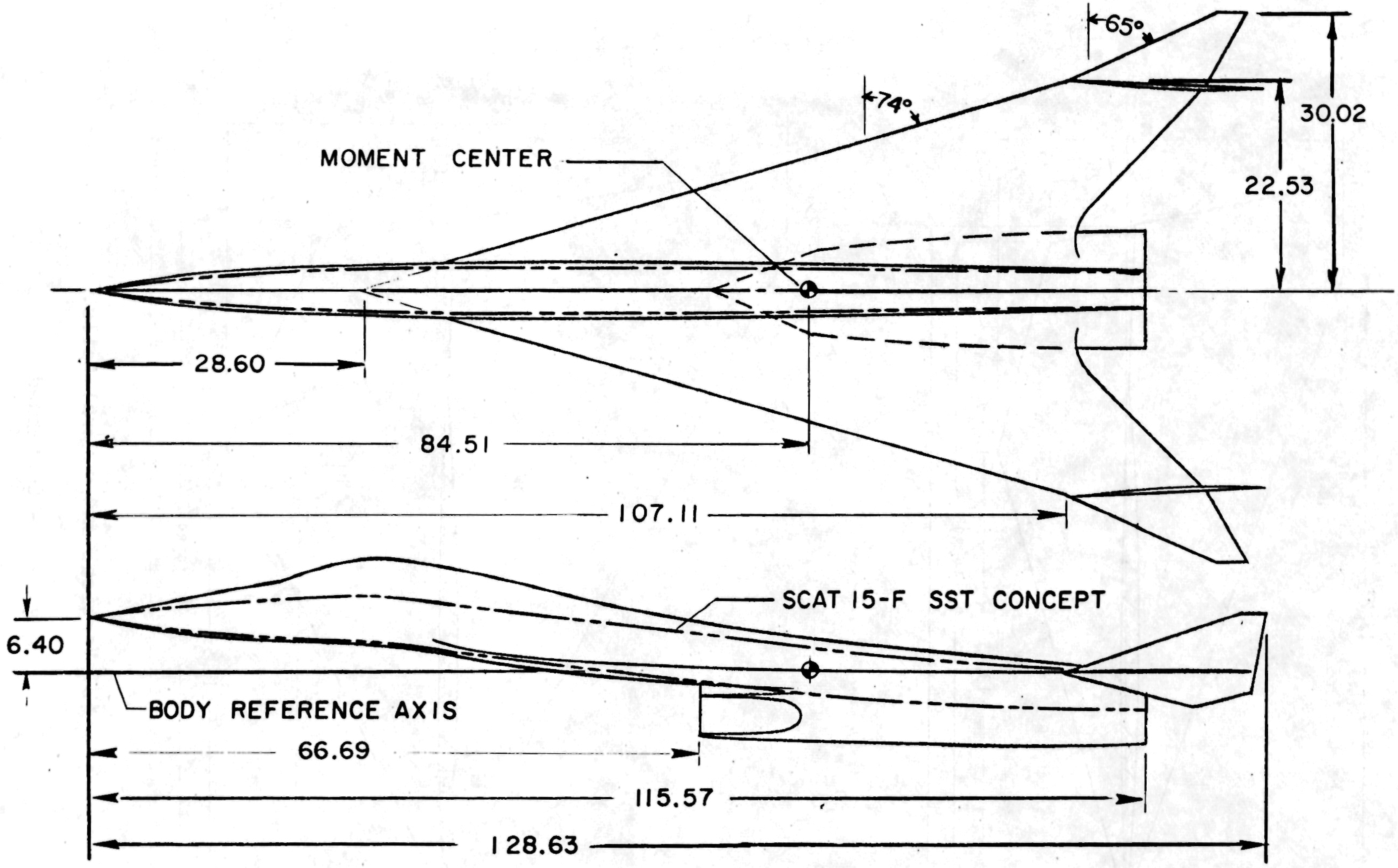

(a) Complete configuration.

Figure 1.- Details of model (dashed line shows SCAT 15F - supersonic transport concept). All linear dimensions are in centimeters.

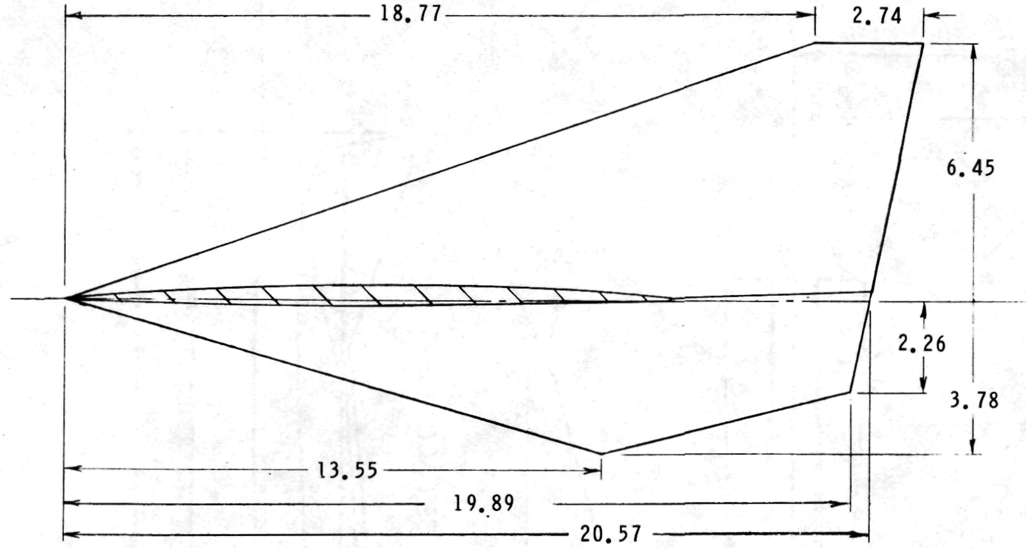

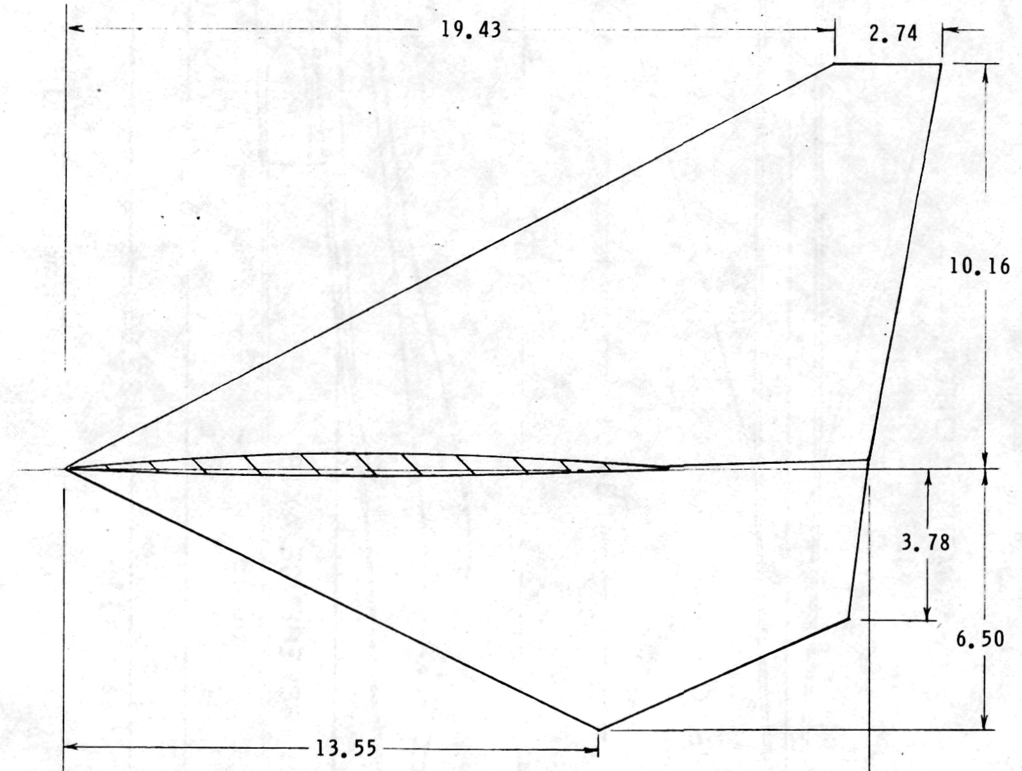

(b) Vertical and ventral tails.

Figure 1.- Continued.

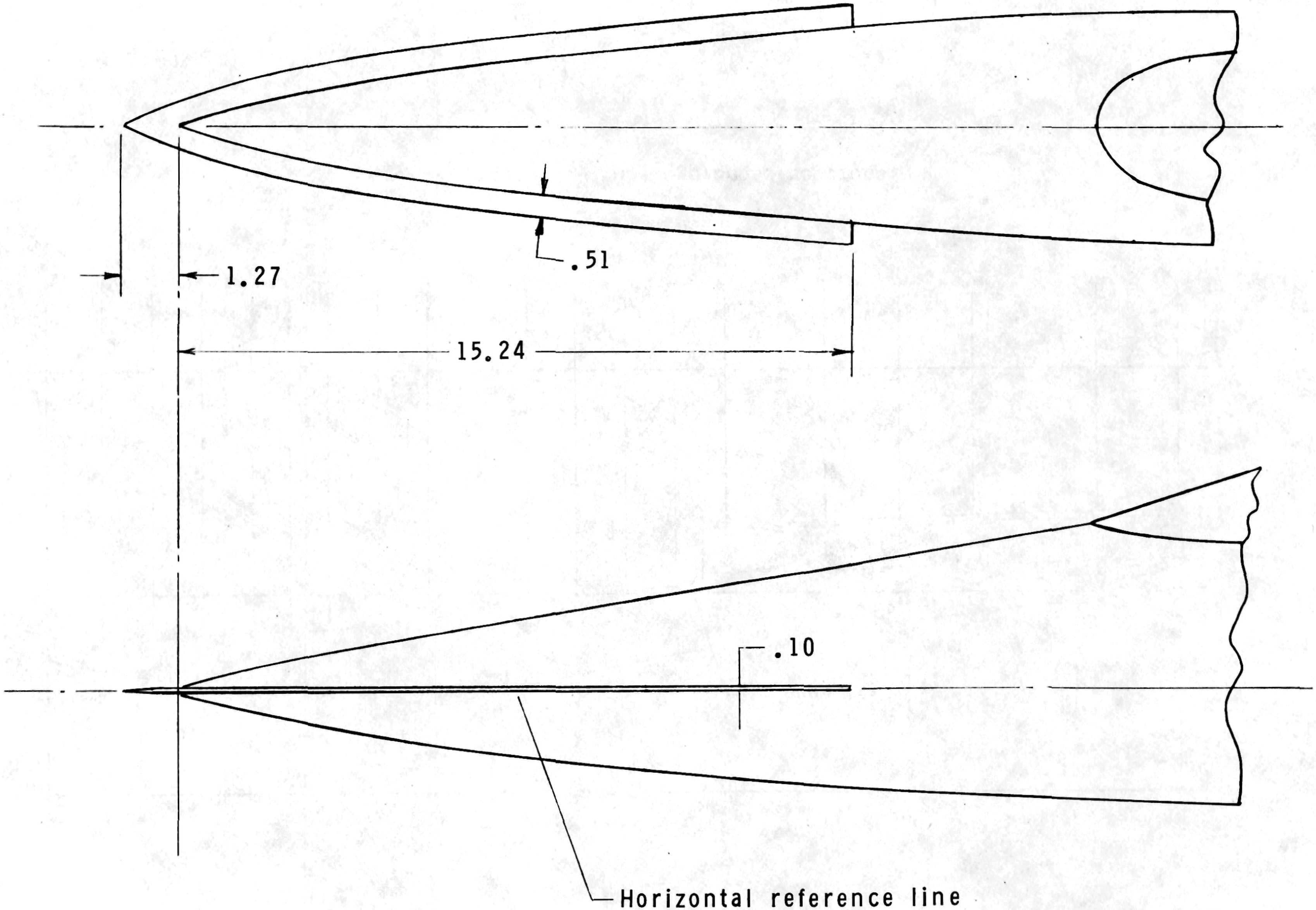

(c) Nose strakes.

Figure 1.- Concluded.

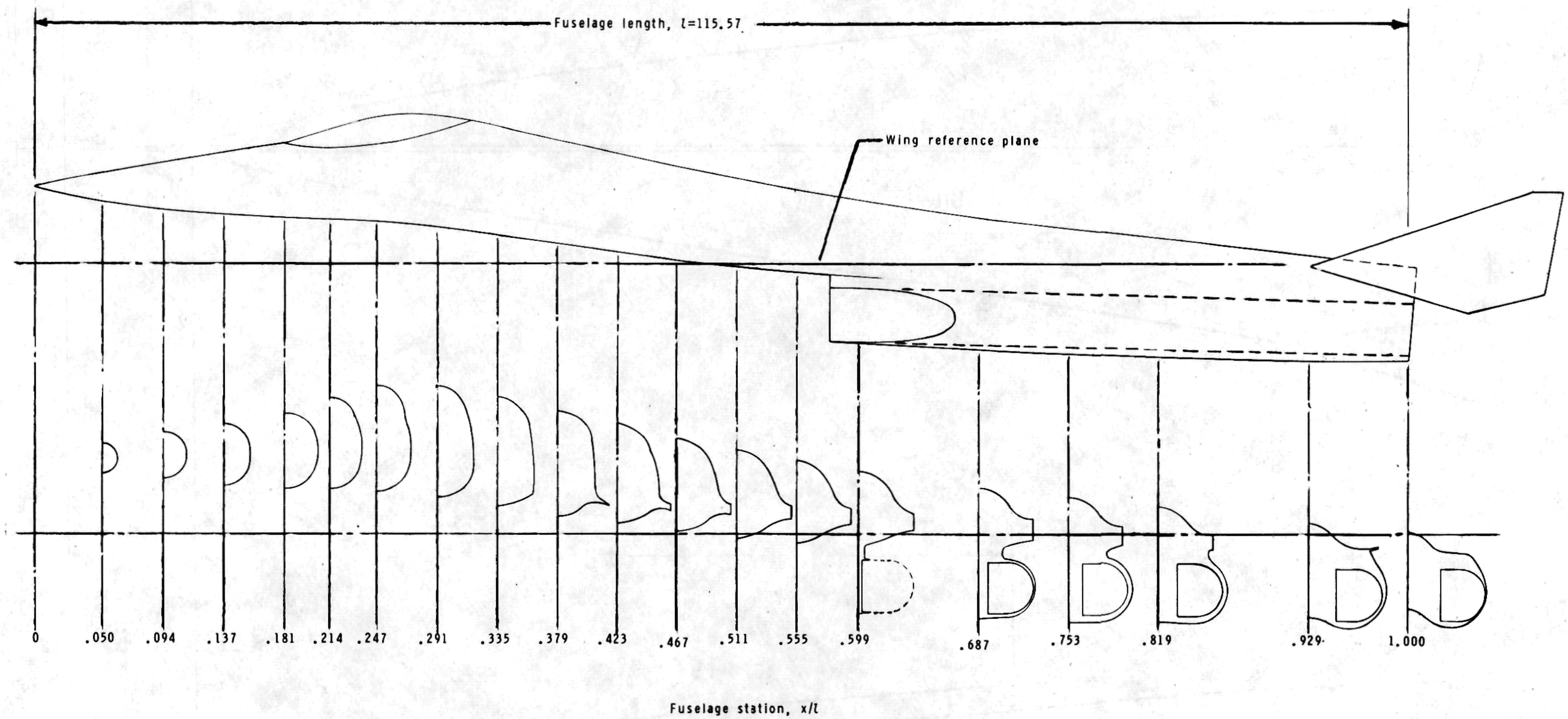

Figure 2.- Fuselage cross sections.

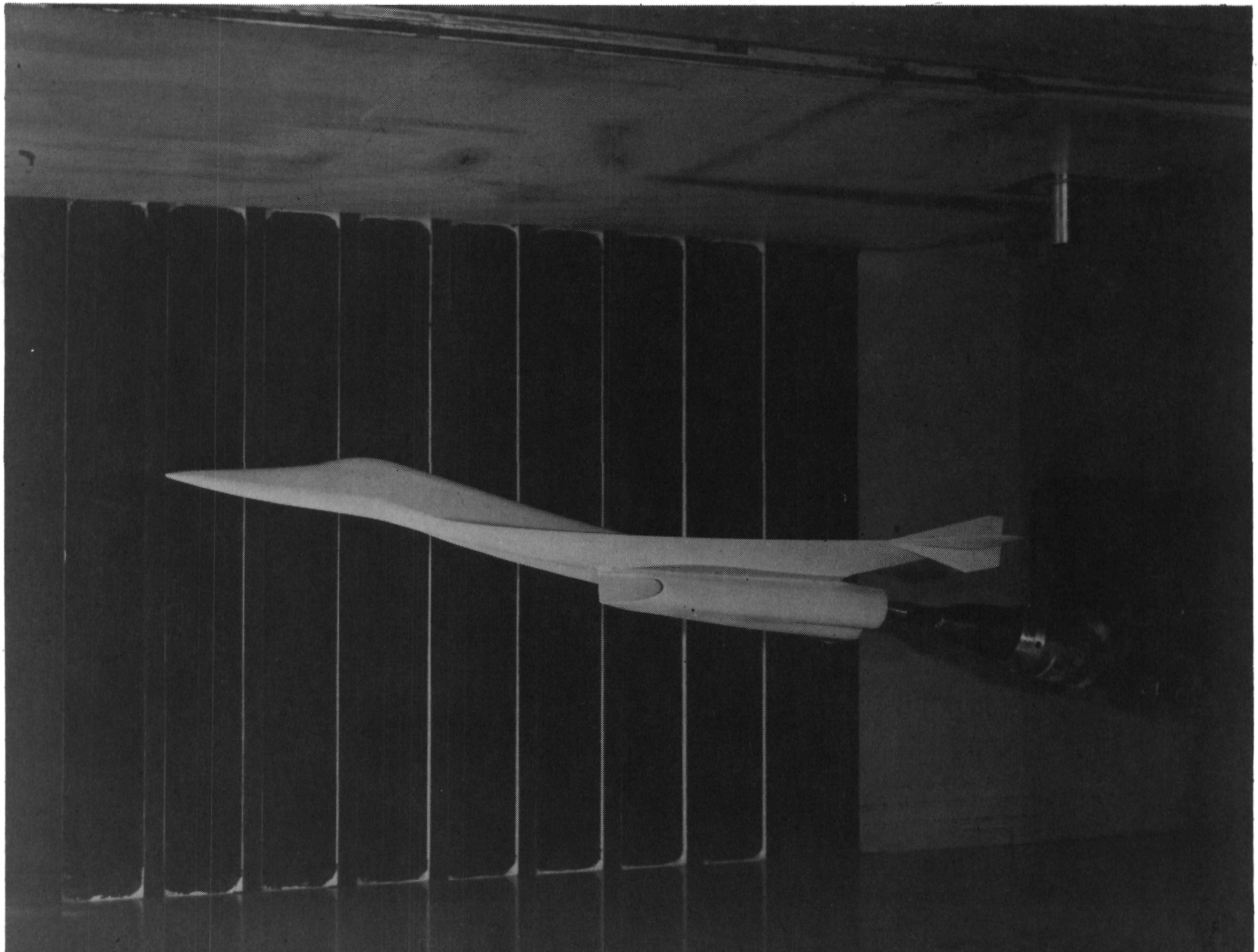

L-76-817

Figure 3.- Photograph of test model in Langley Unitary Plan wind tunnel.

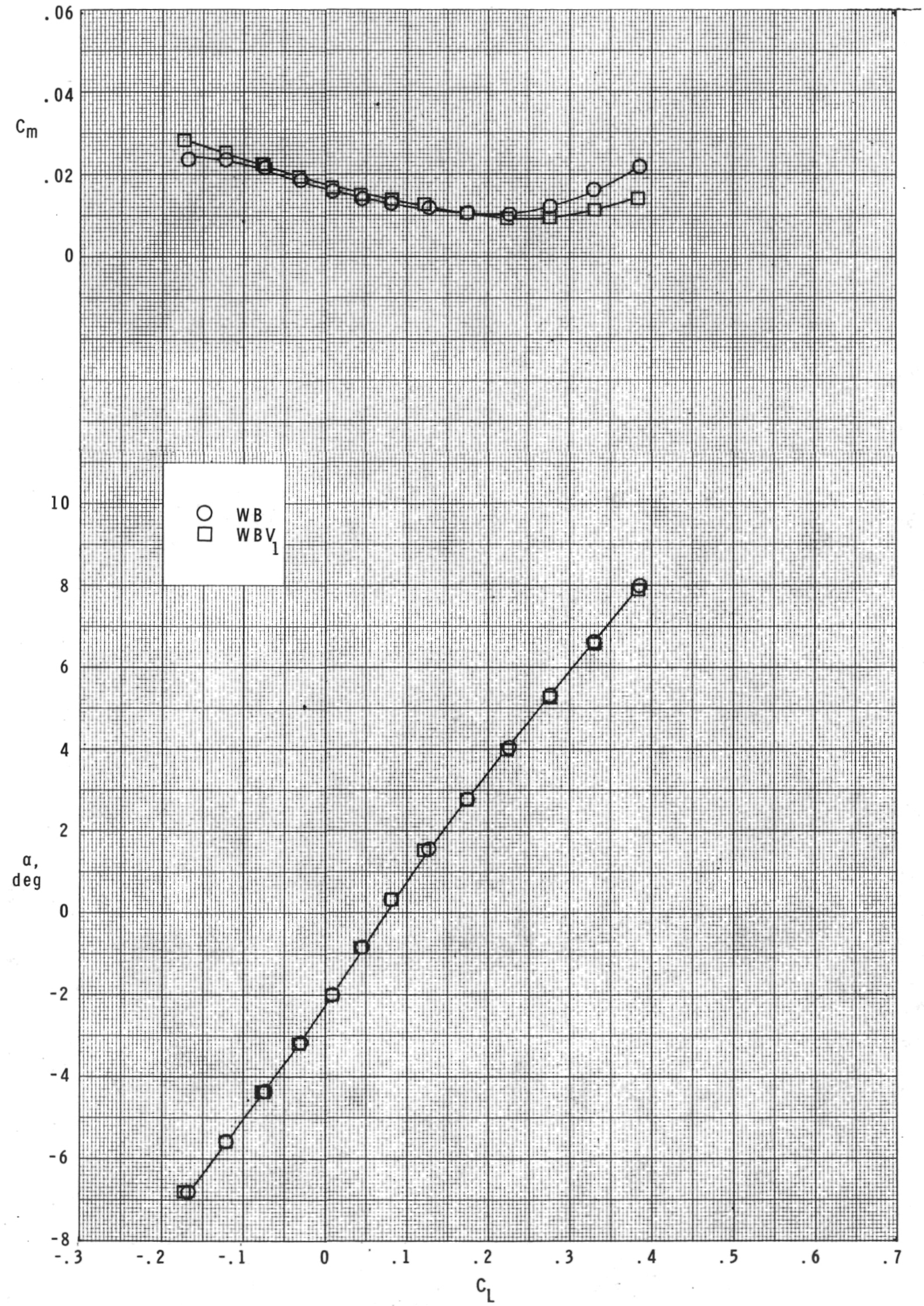

(a) M = 0.60.

Figure 4.- Comparison of longitudinal aerodynamic characteristics in pitch for complete basic model configuration with and without small vertical and ventral tails.

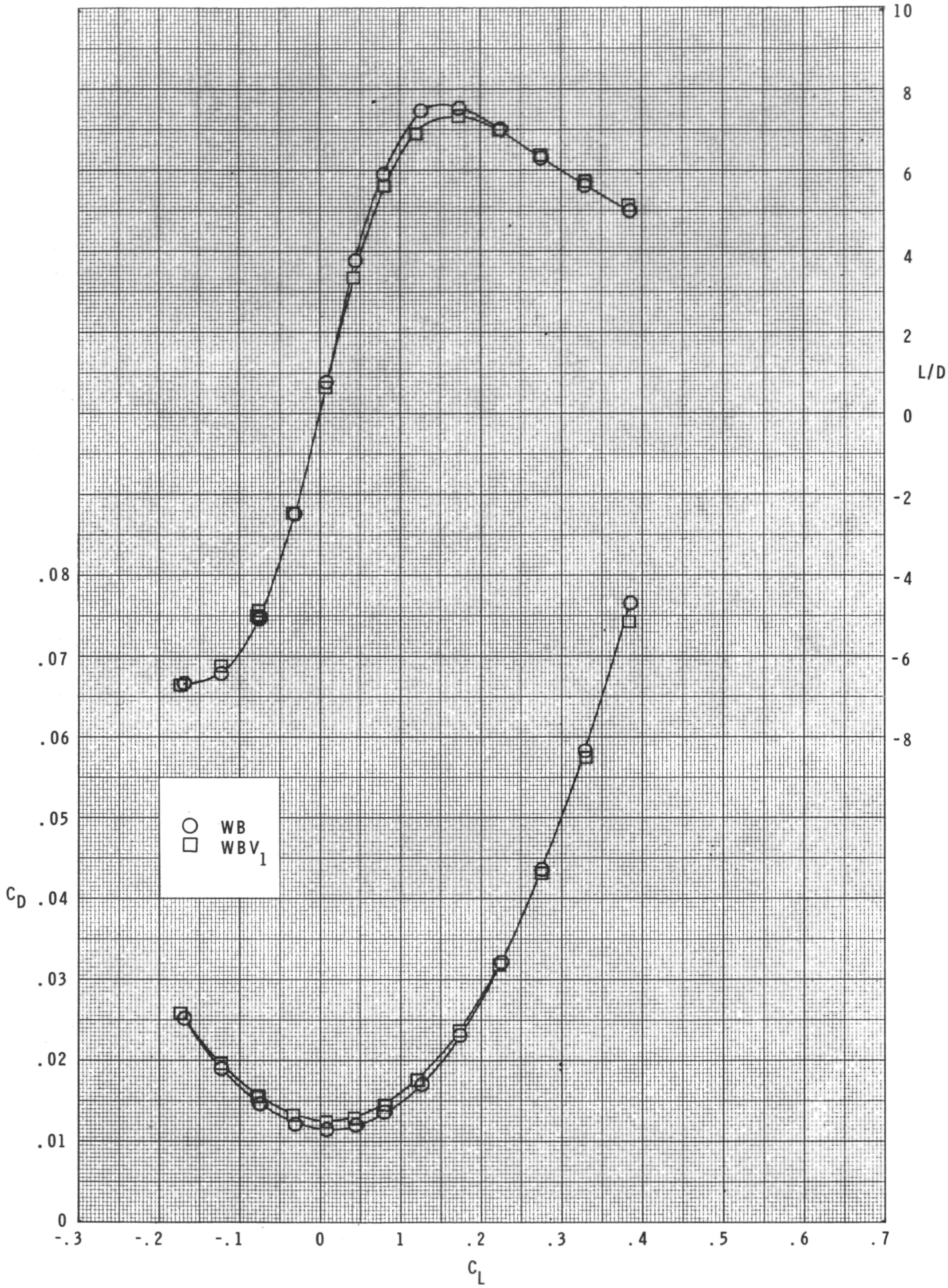

(a) M = 0.60, concluded.

Figure 4.- Continued.

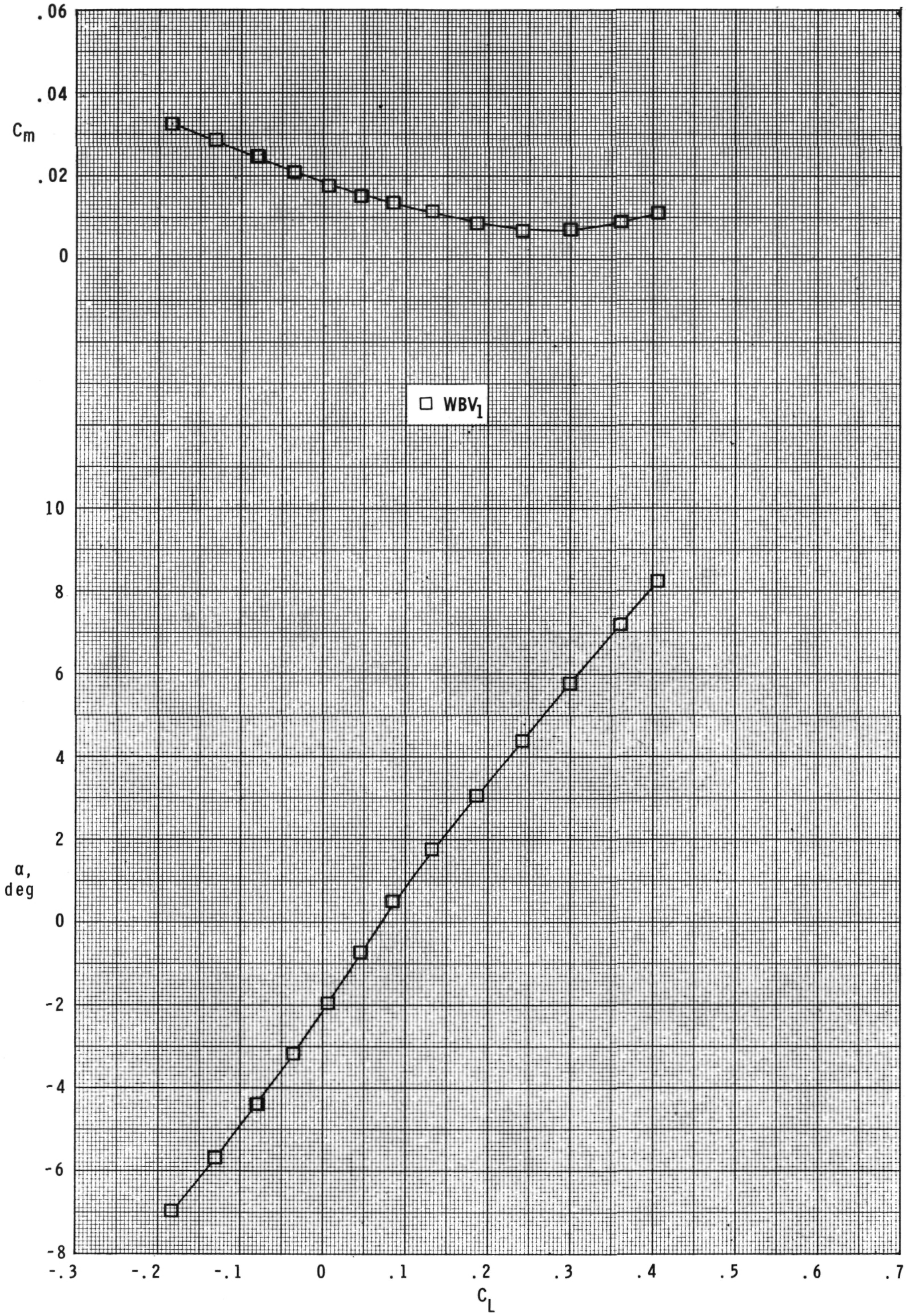

(b) M = 0.80. (Data for complete model only.)

Figure 4.- Continued.

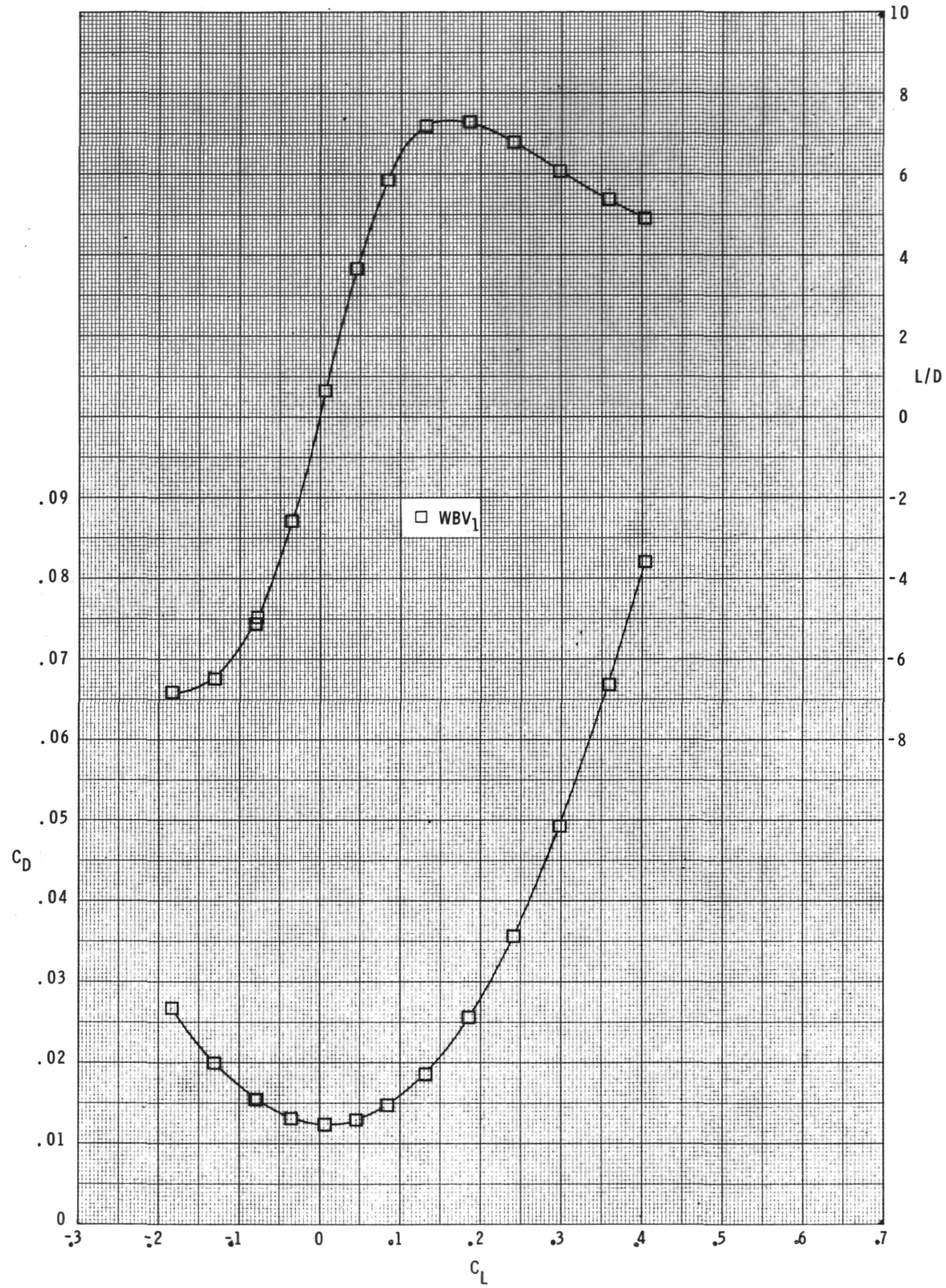

(b) M = 0.80, concluded. (Data for complete model only.)

Figure 4.- Continued.

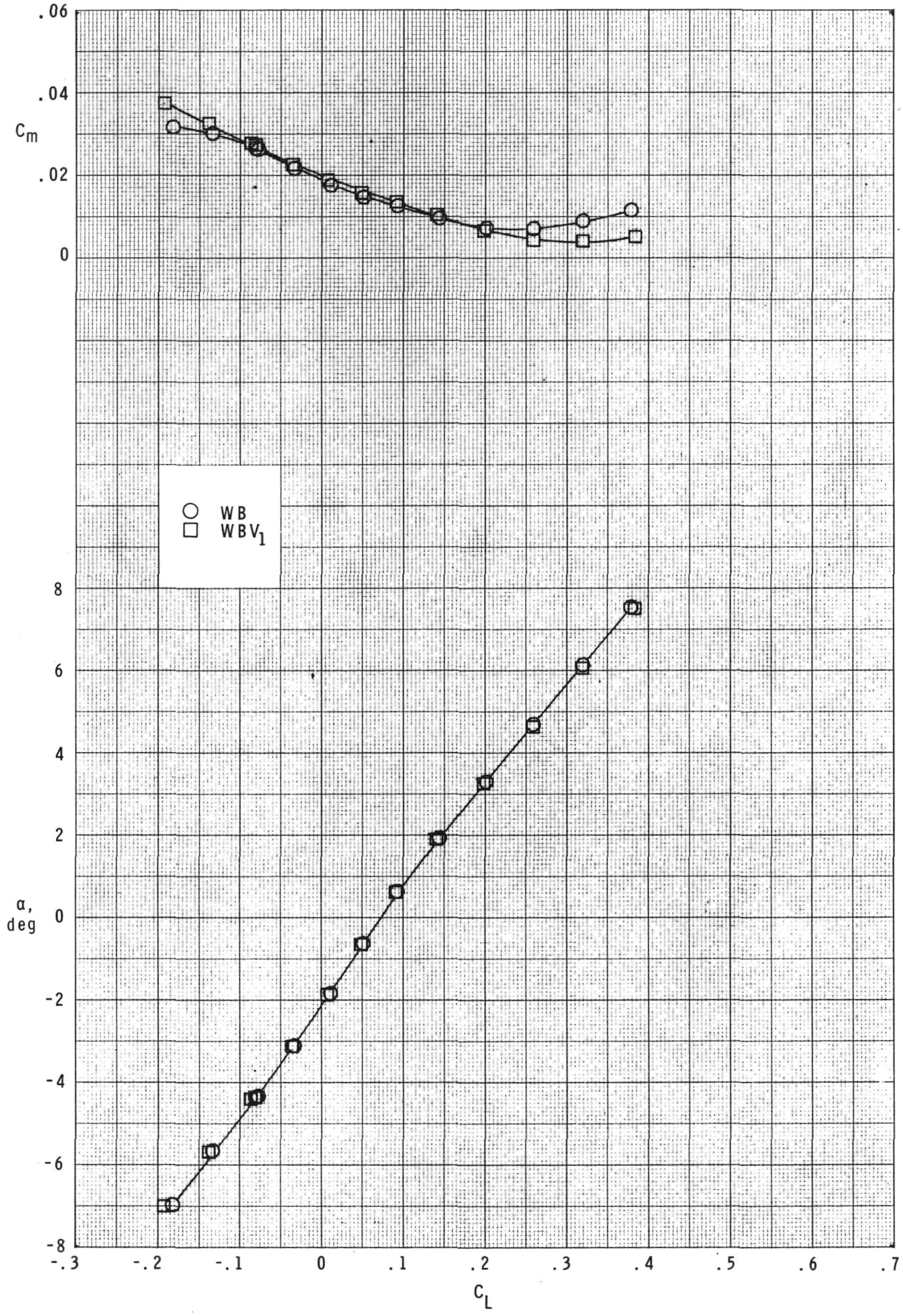

(c) M = 0.90.

Figure 4.- Continued.

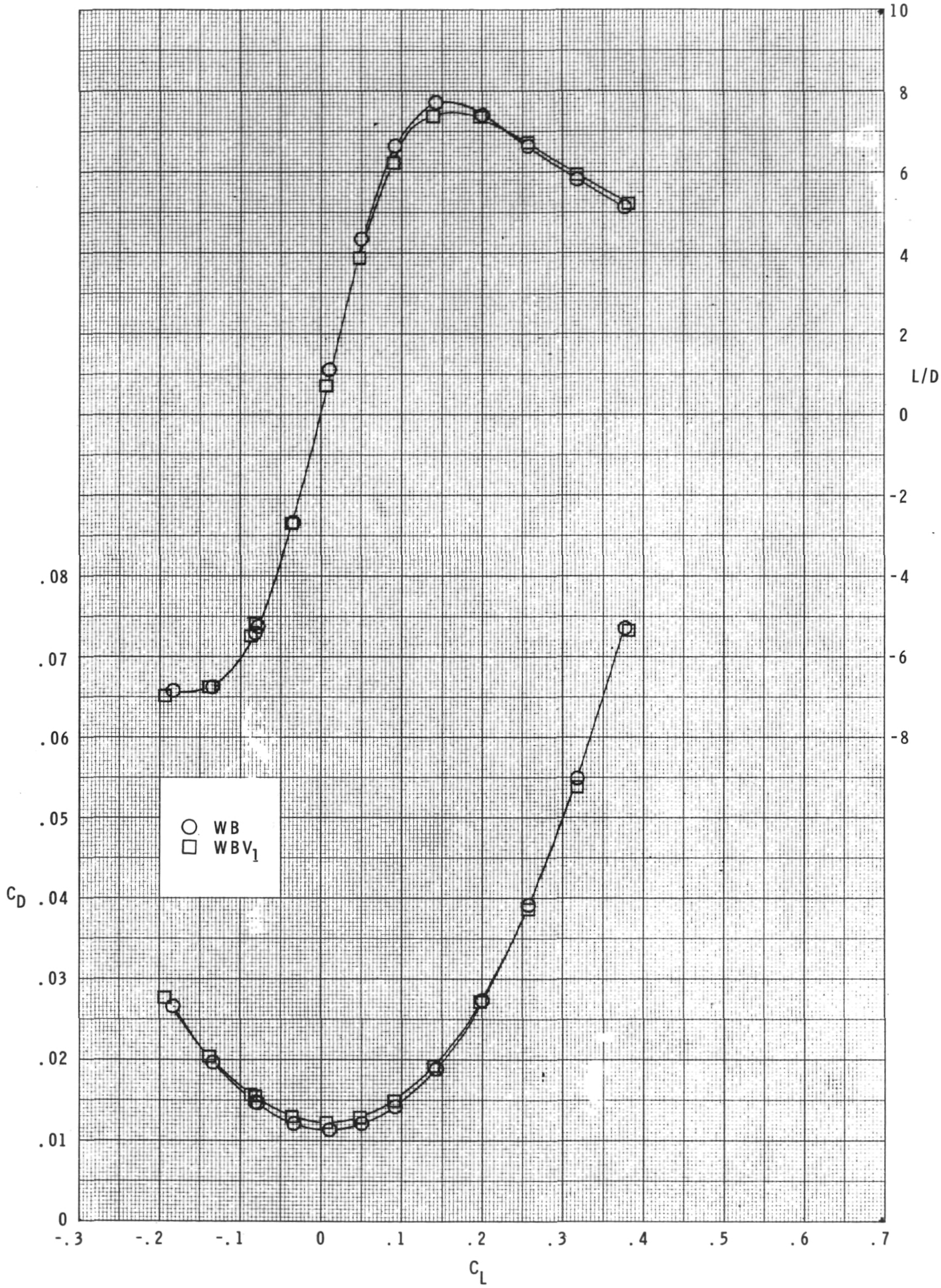

(c) M = 0.90, concluded.

Figure 4.- Continued.

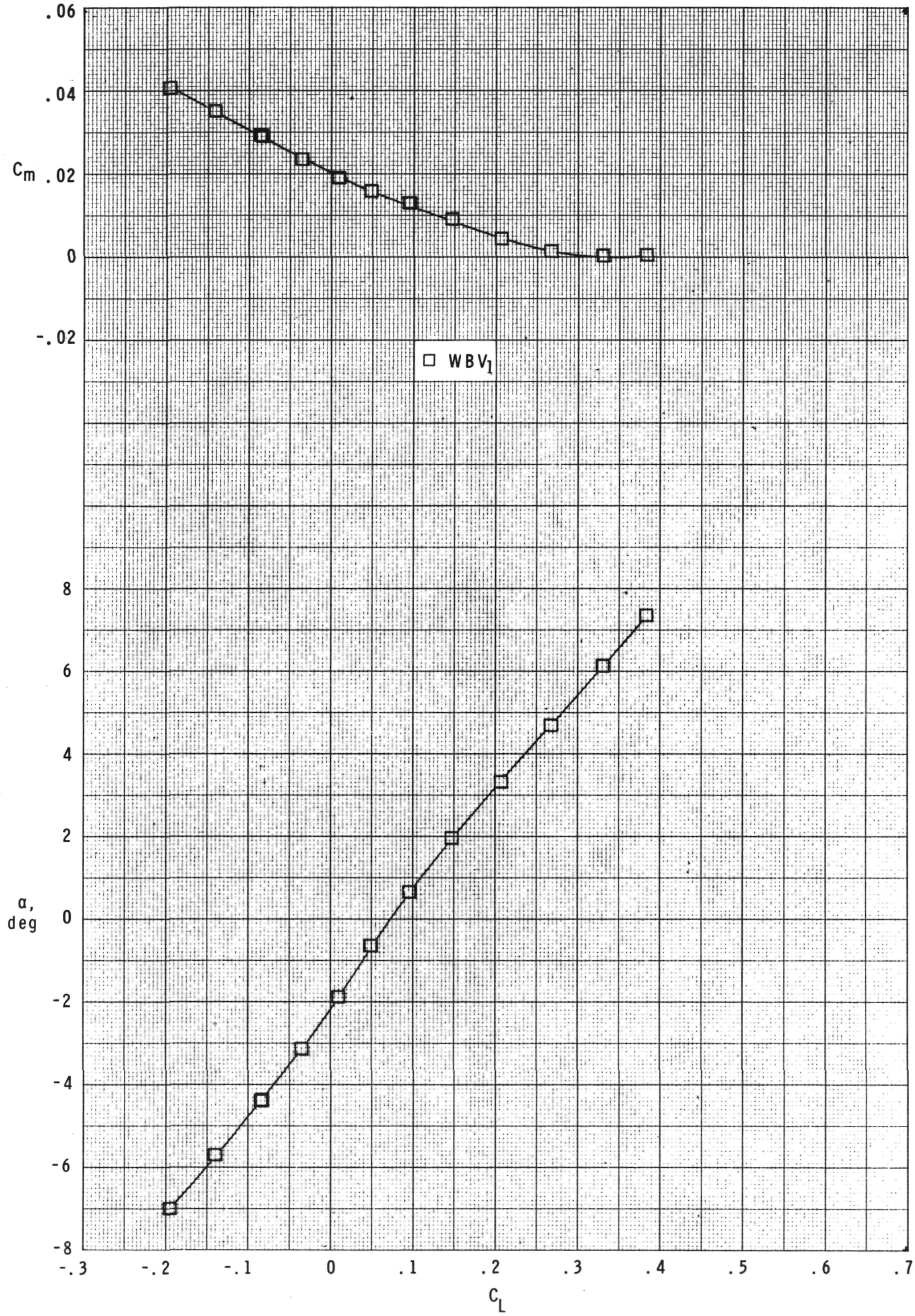

(d) M = 0.95. (Data for complete model only.)

Figure 4.- Continued.

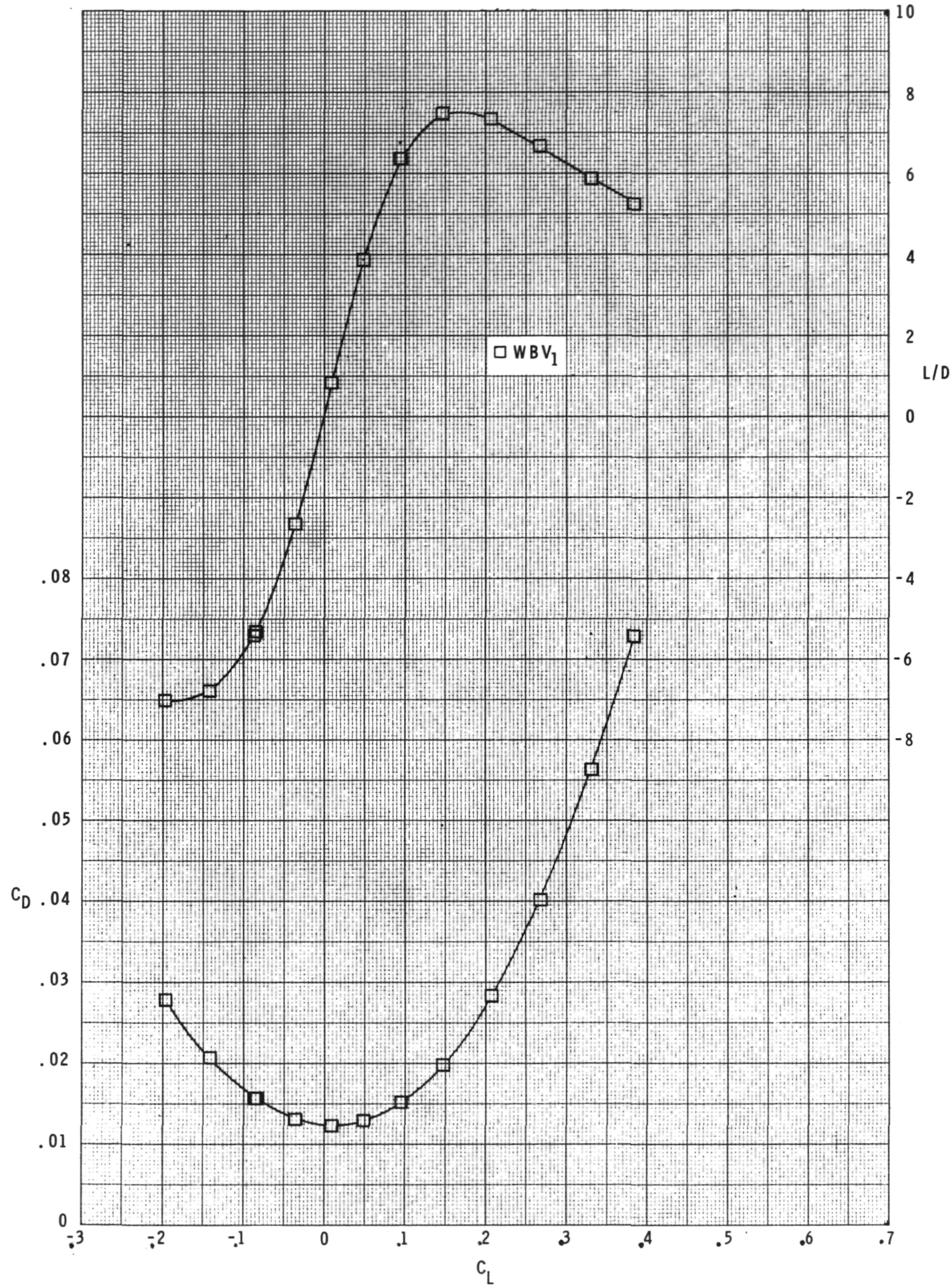

(d) M = 0.95, concluded. (Data for complete model only.)

Figure 4.- Continued.

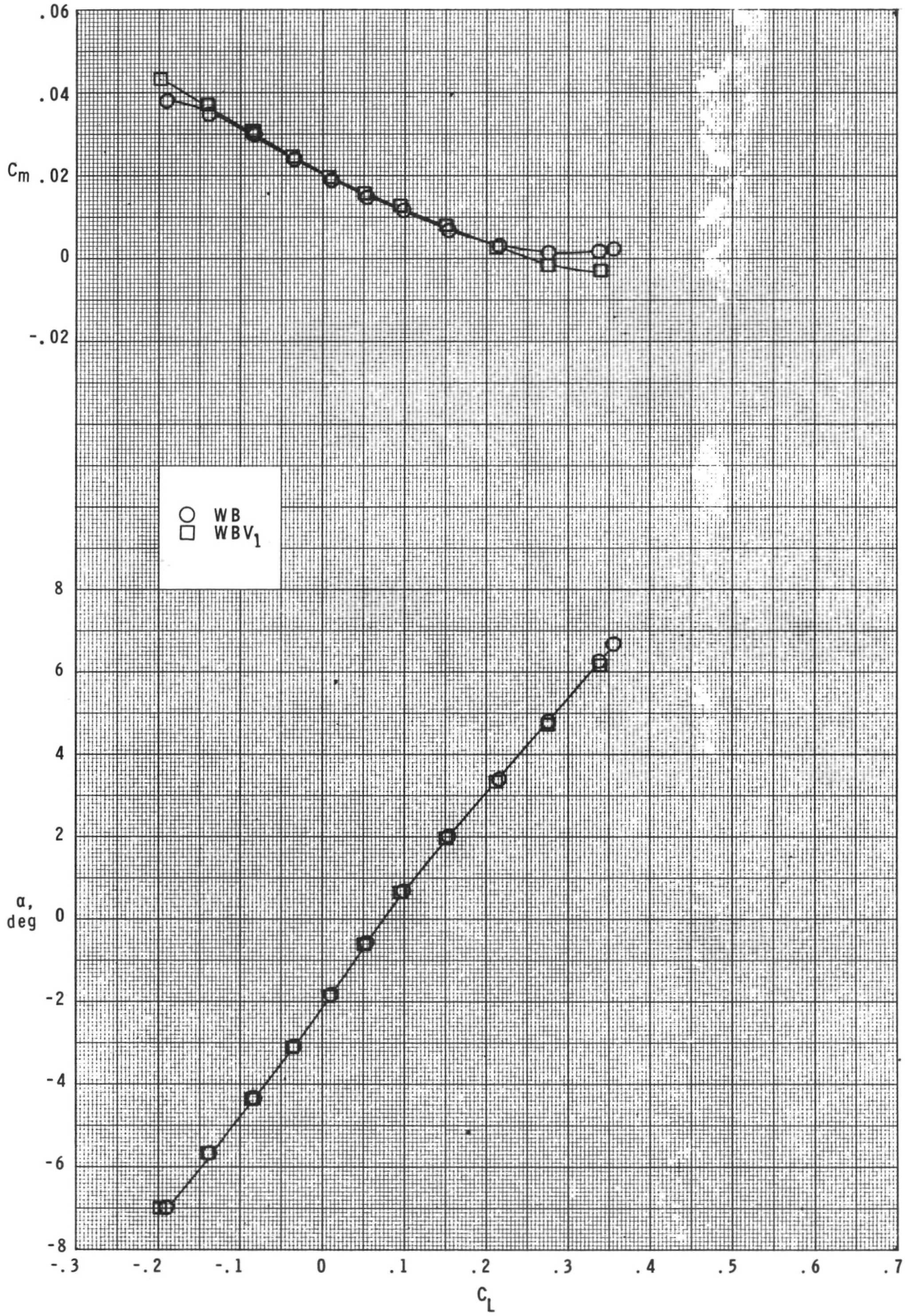

(e) M = 0.97.

Figure 4.- Continued.

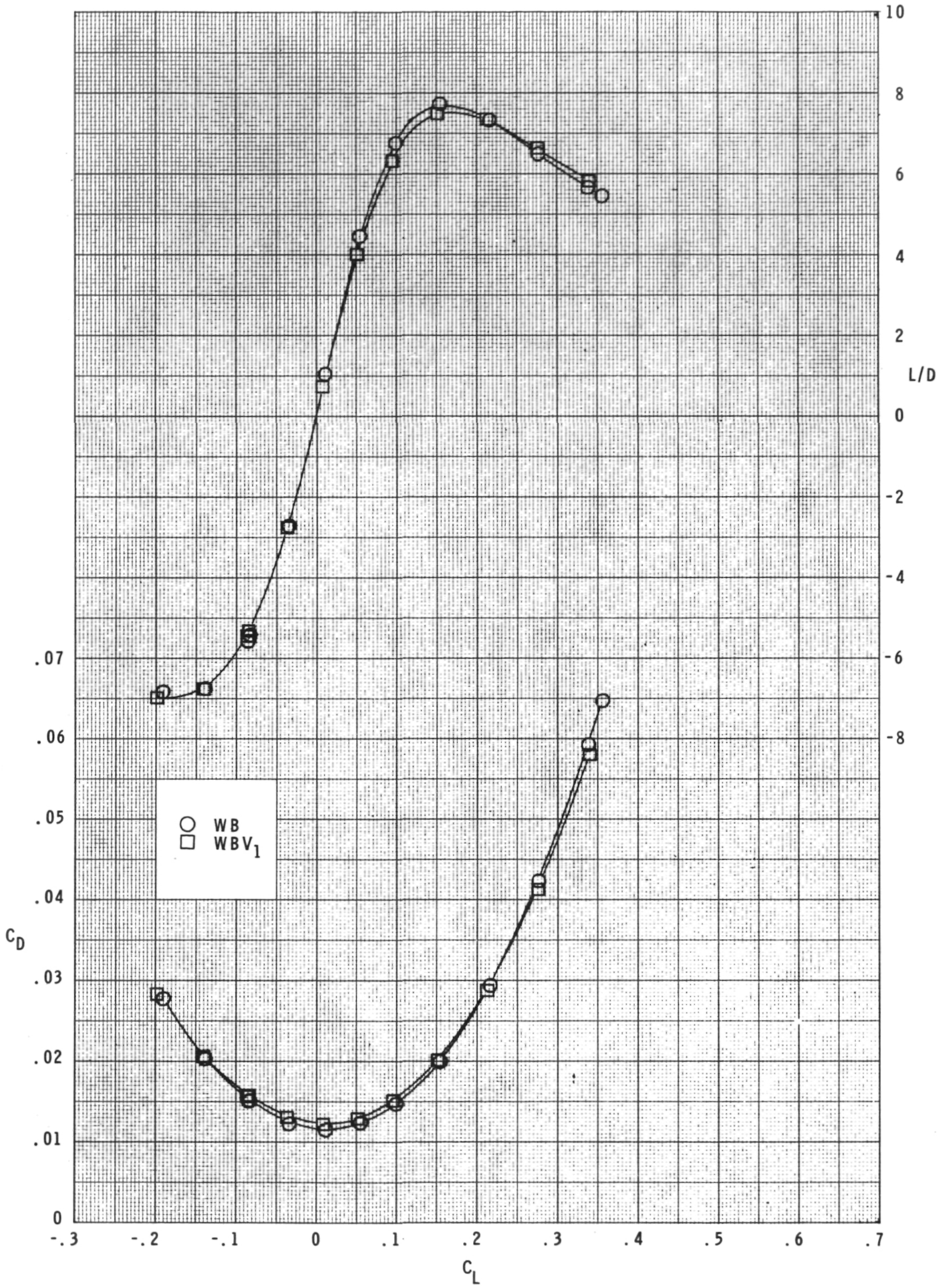

(e) M = 0.97, concluded.

Figure 4.- Continued.

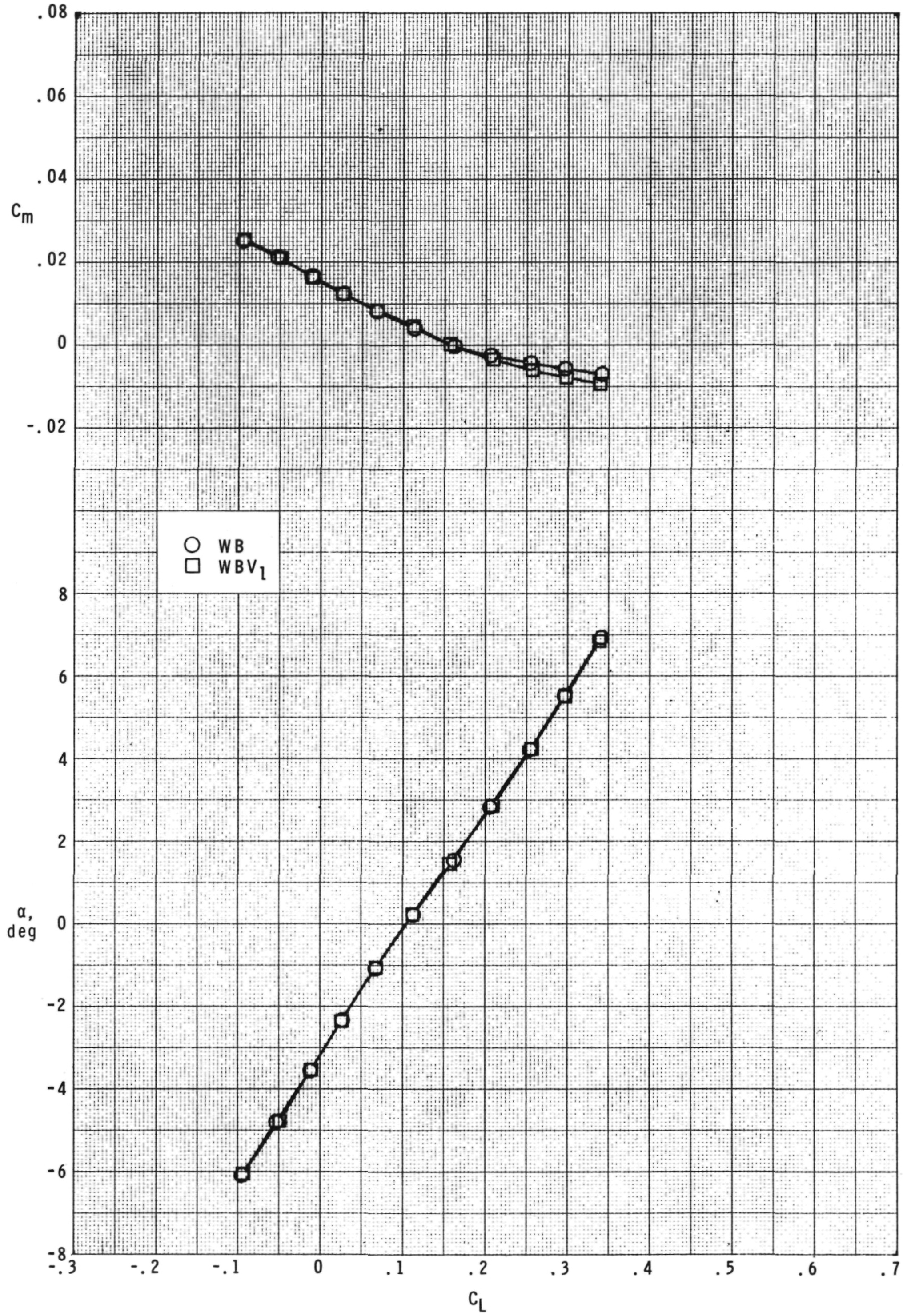

(f) M = 1.80.

Figure 4.- Continued.

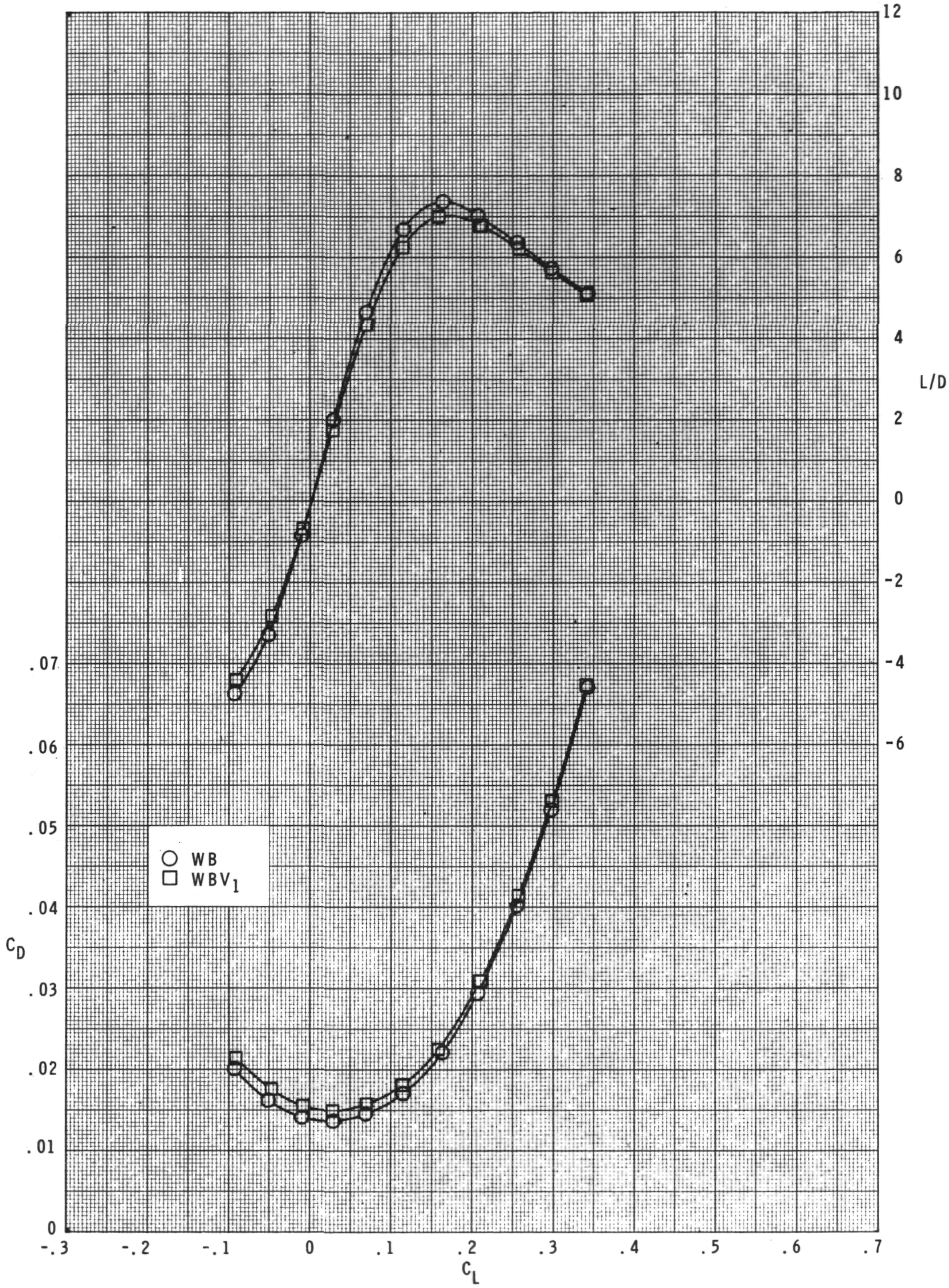

(f) M = 1.80, concluded.

Figure 4.- Continued.

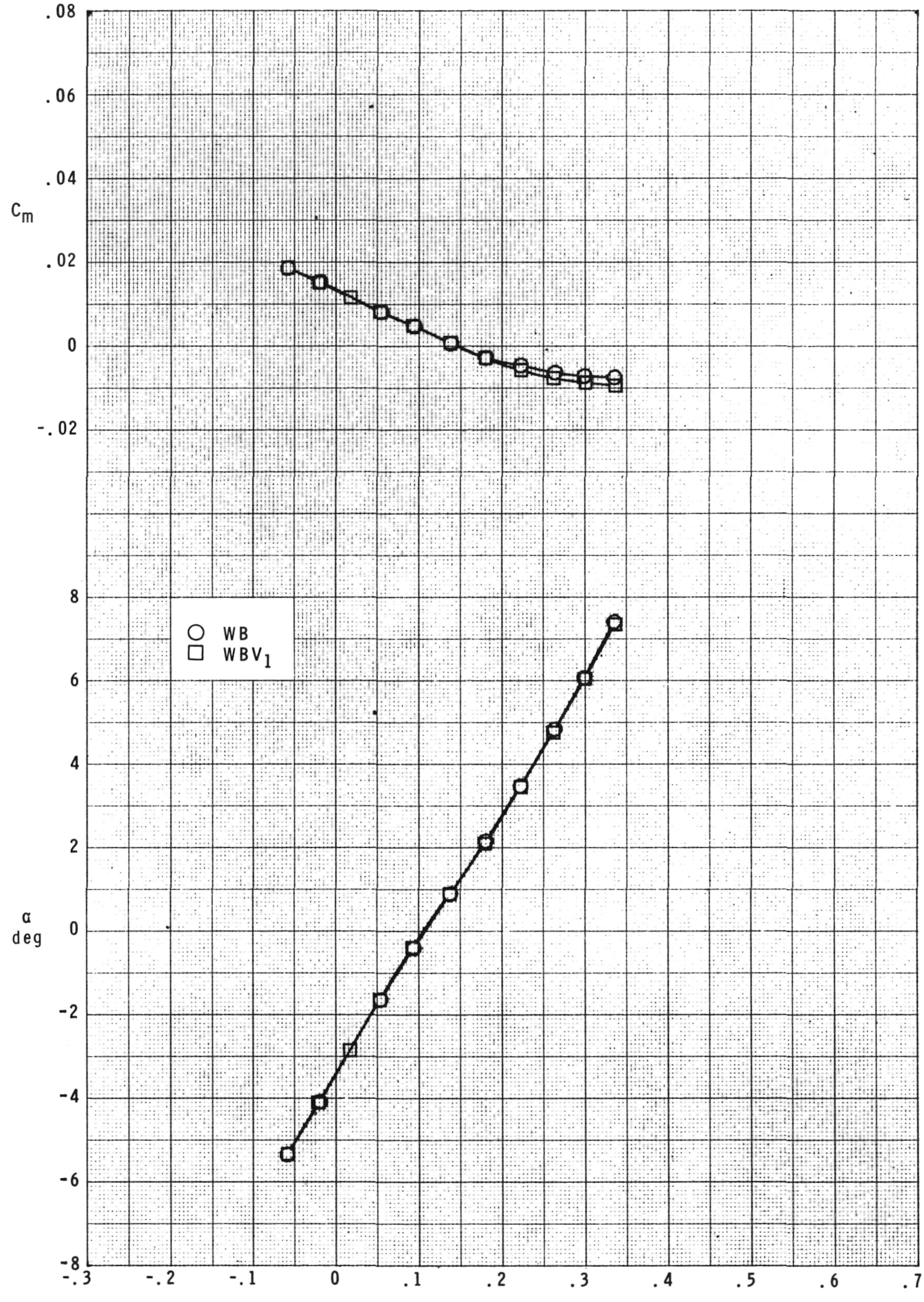

(g) M = 2.00.

Figure 4.- Continued.

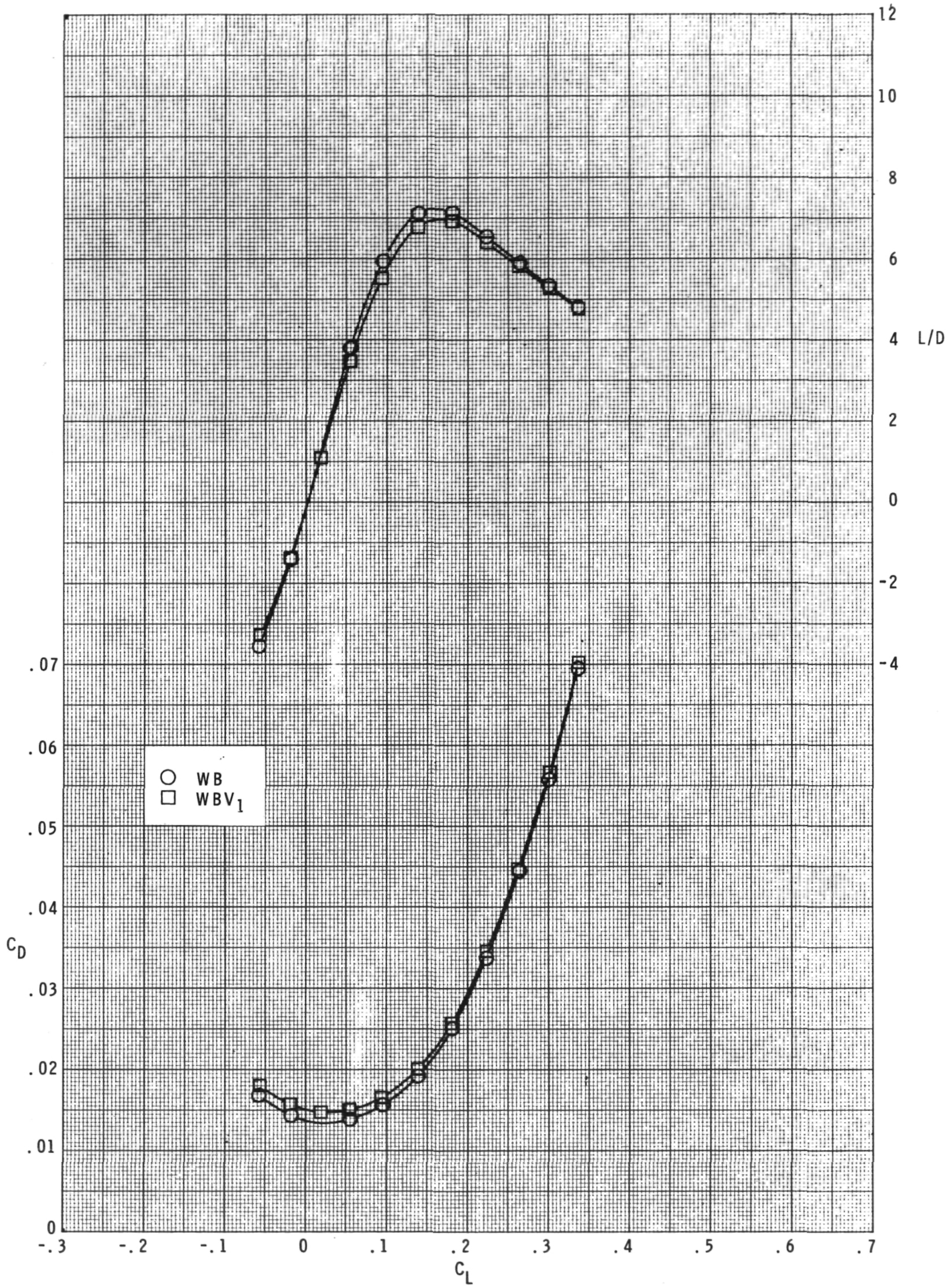

(g) M = 2.00, concluded.

Figure 4.- Continued.

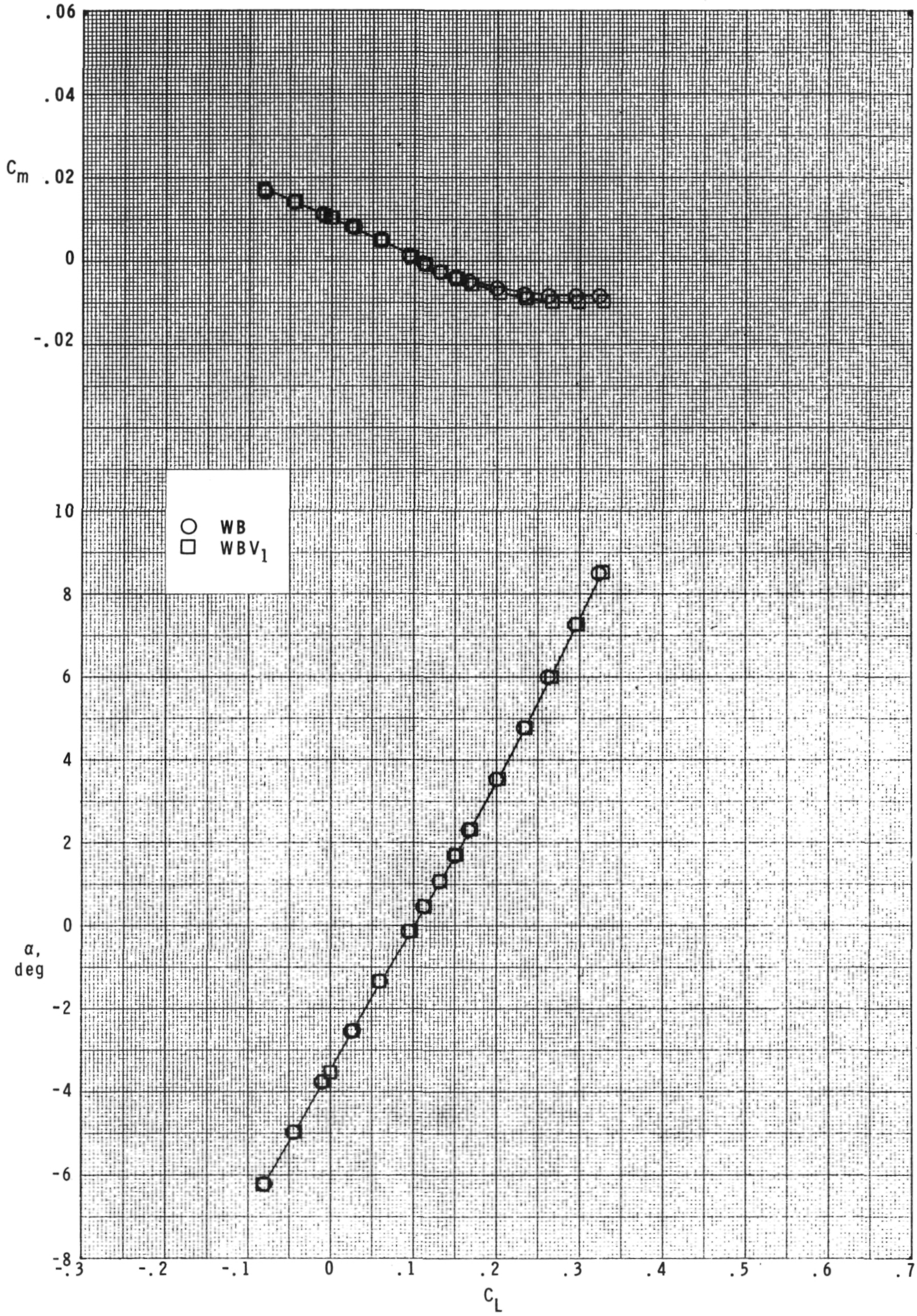

(h) M = 2.30.

Figure 4.- Continued.

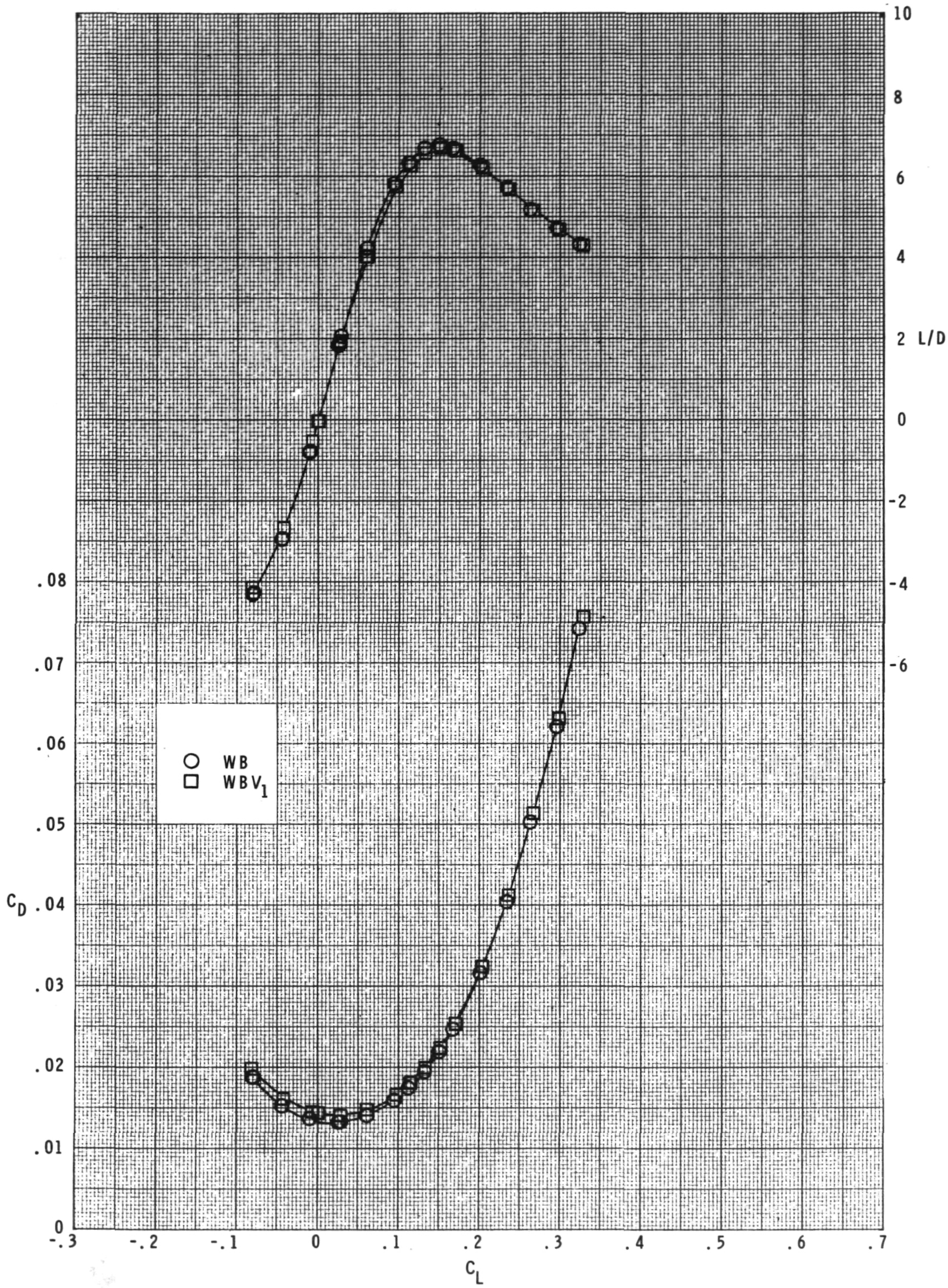

(h) M = 2.30, concluded.

Figure 4.- Continued.

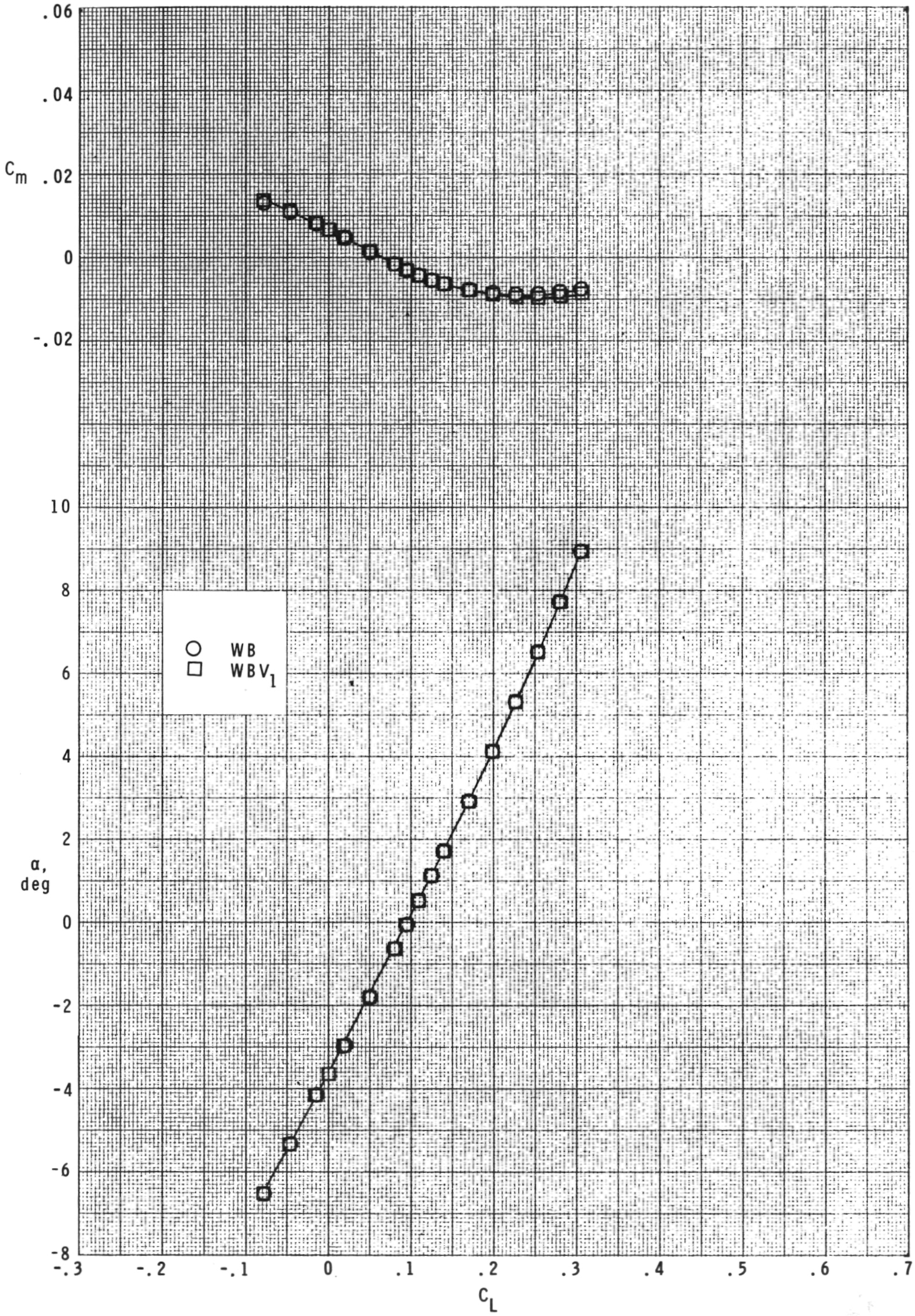

(i) M = 2.60.

Figure 4.- Continued.

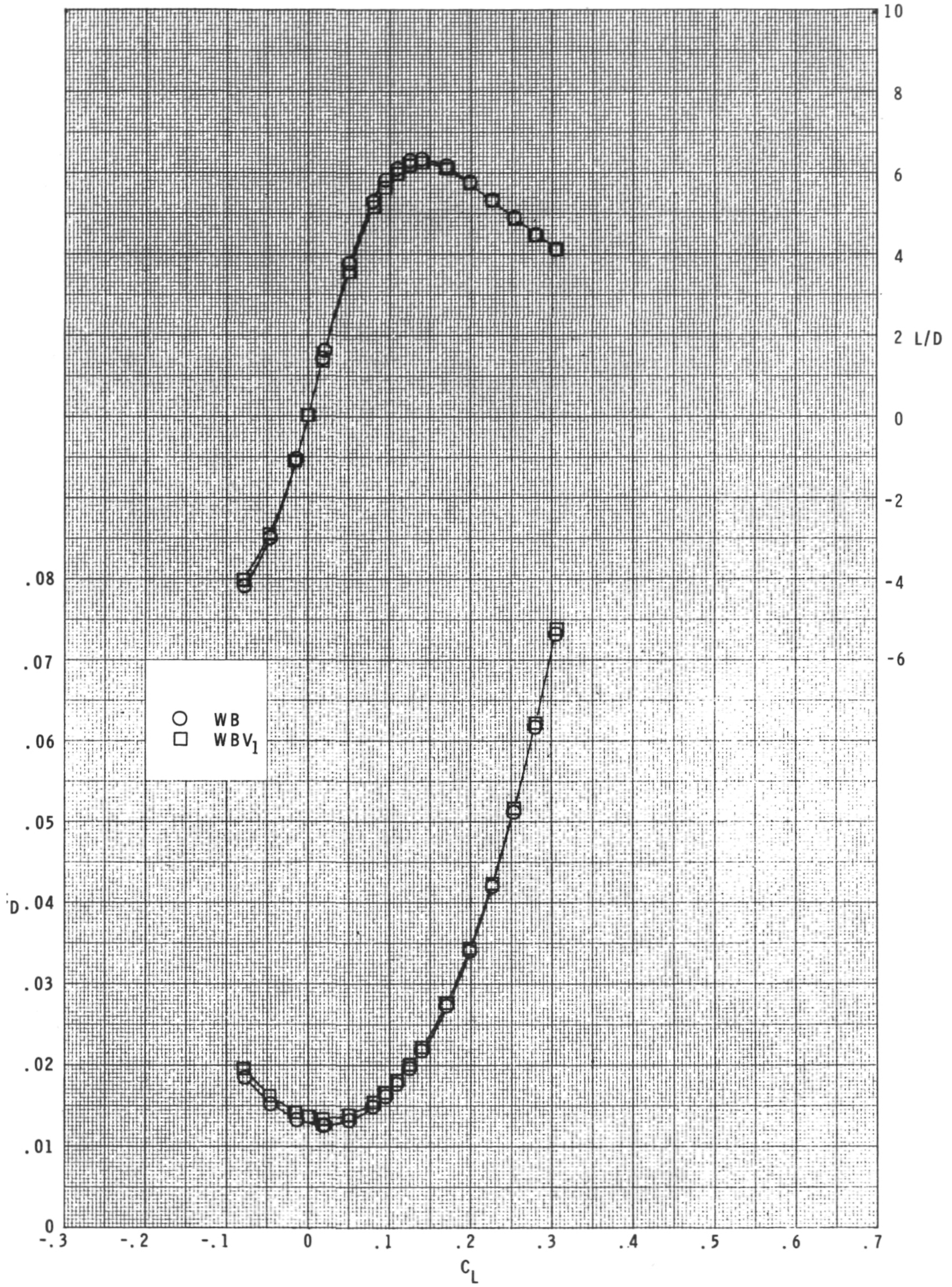

(i) M = 2.60, concluded.

Figure 4.- Continued.

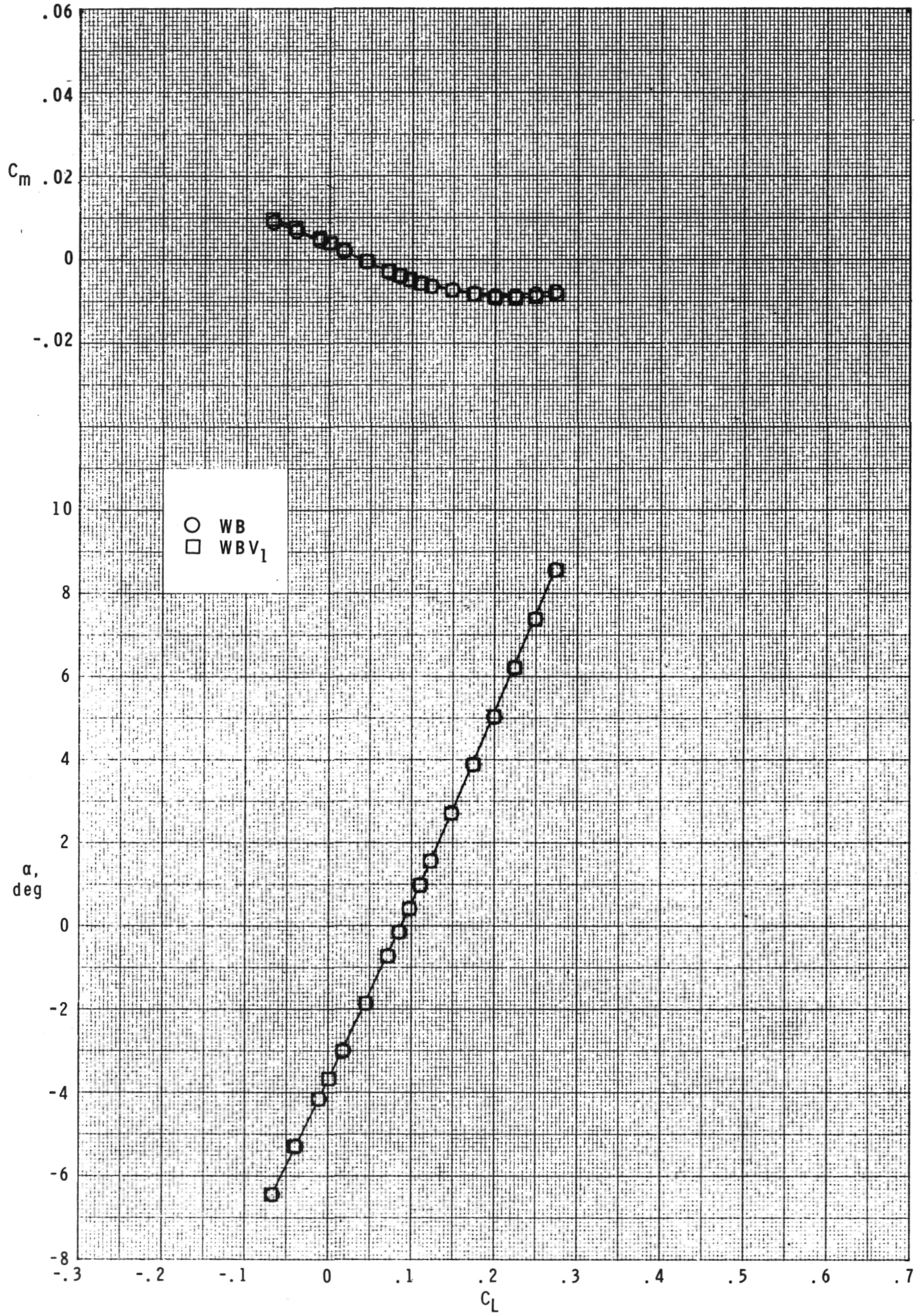

(j) M = 2.96.

Figure 4.- Continued.

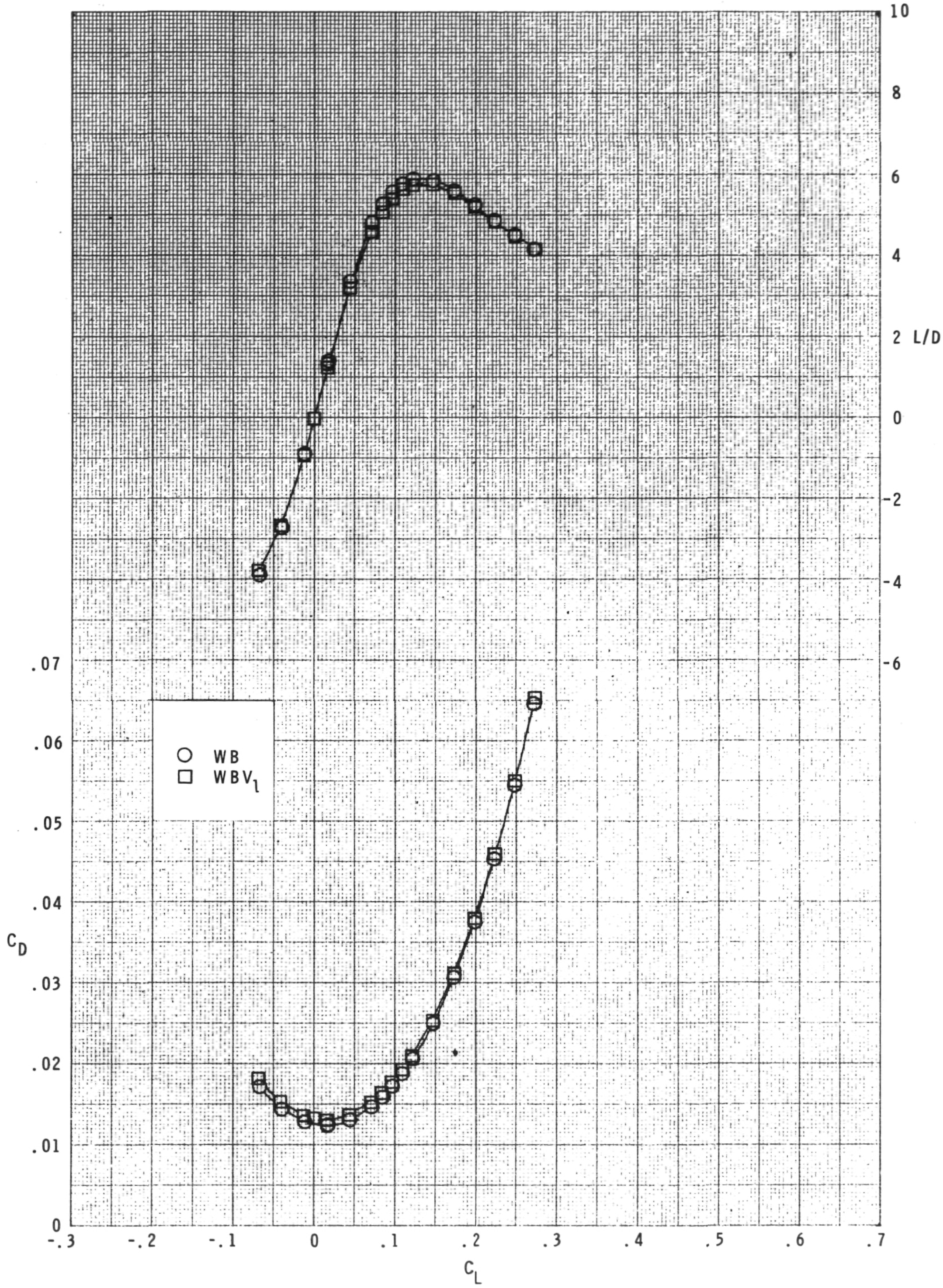

(j) M = 2.96, concluded.

Figure 4.- Concluded.

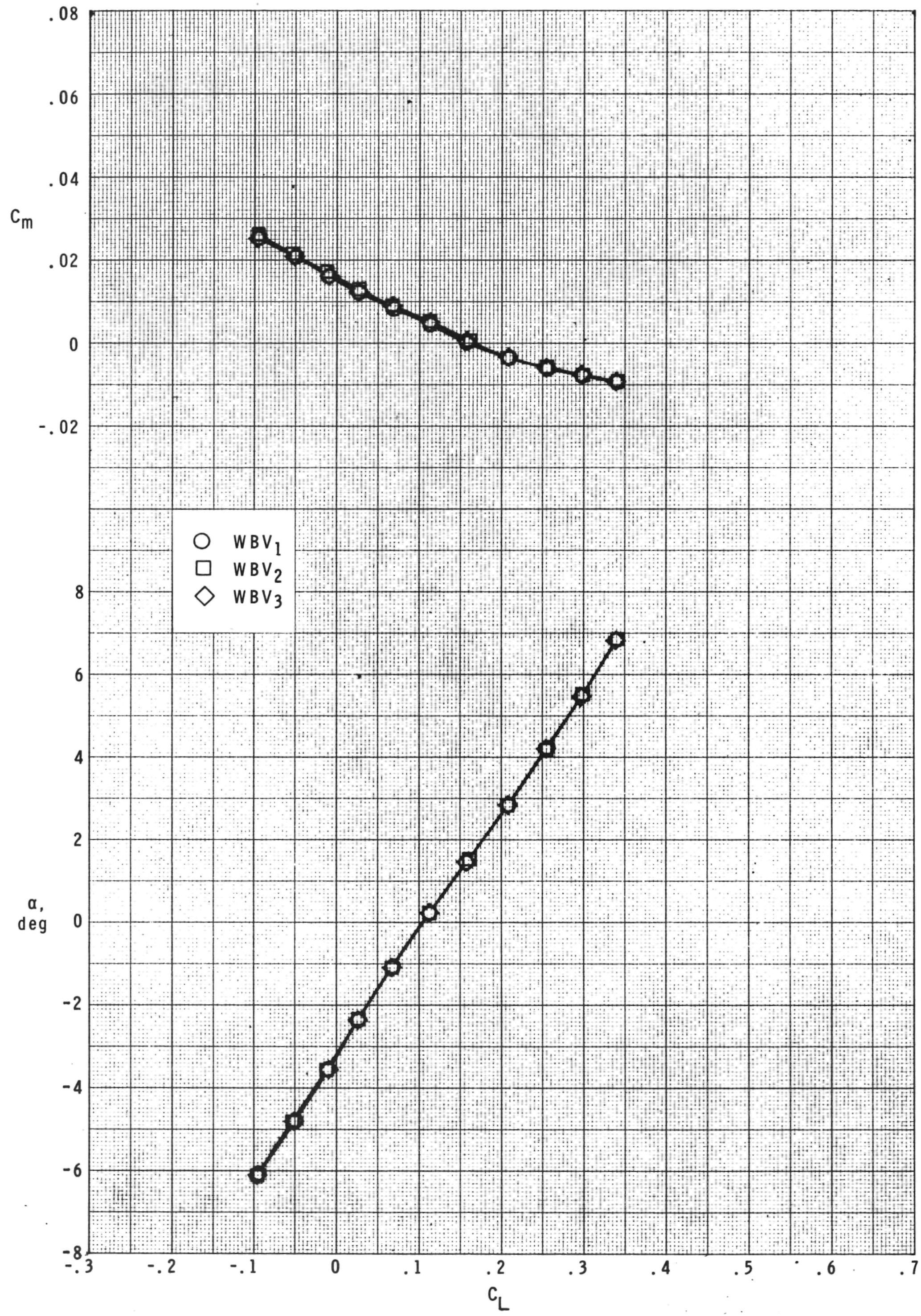

(a) M = 1.80.

Figure 5.- Effect of vertical and ventral tail size on aerodynamic characteristics in pitch.

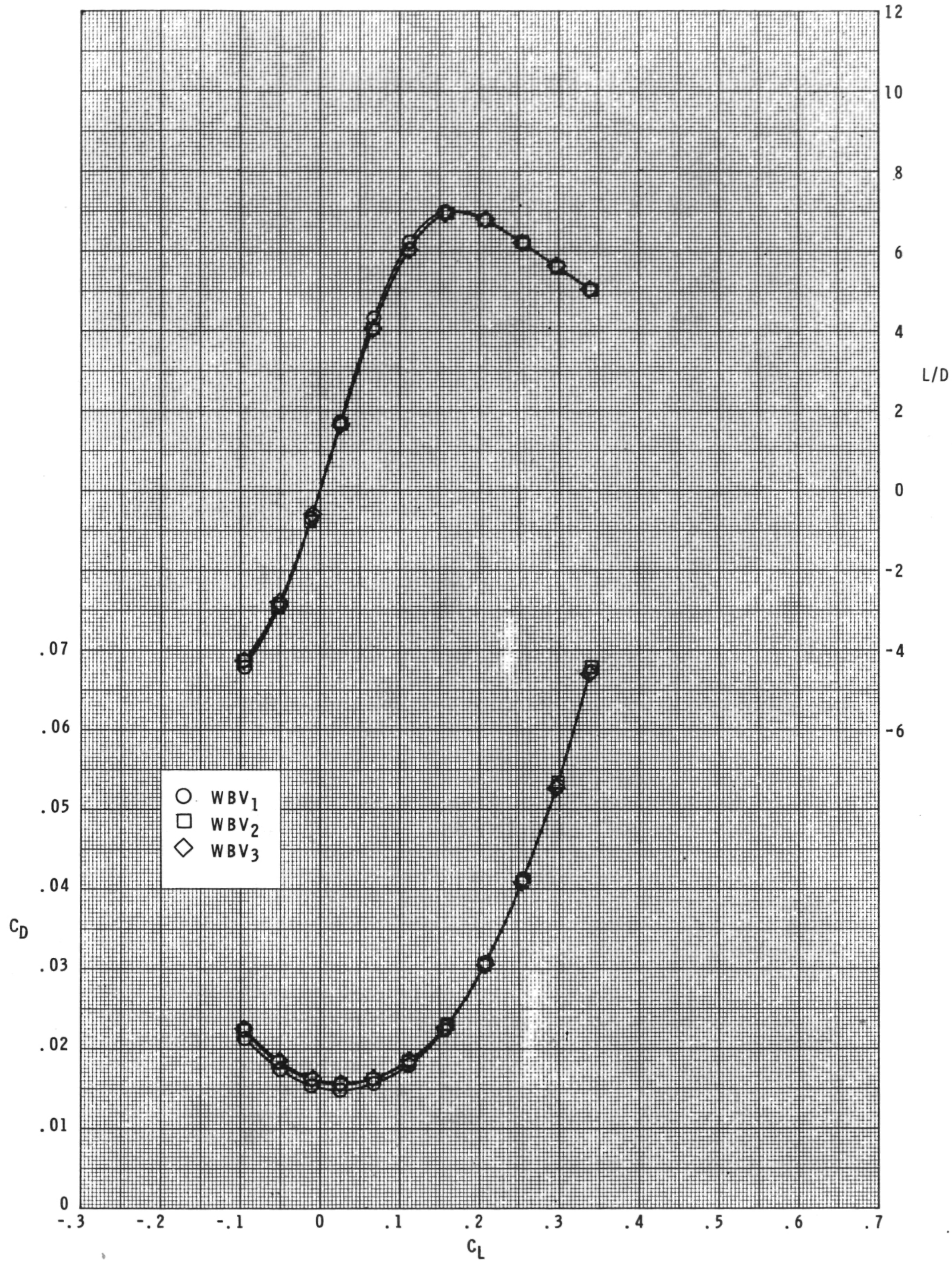

(a) M = 1.80, concluded.

Figure 5.- Continued.

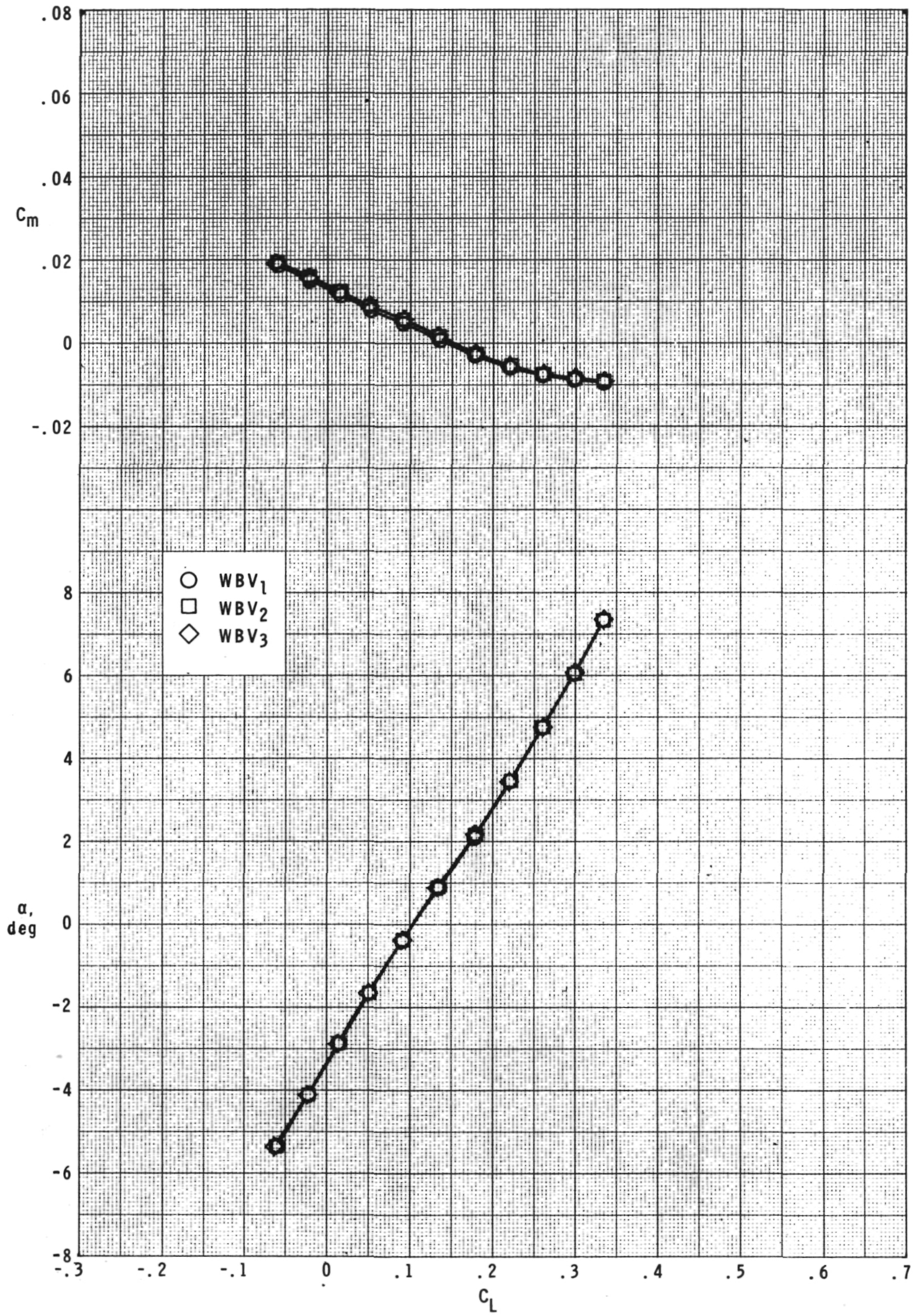

(b) M = 2.00.

Figure 5.- Continued.

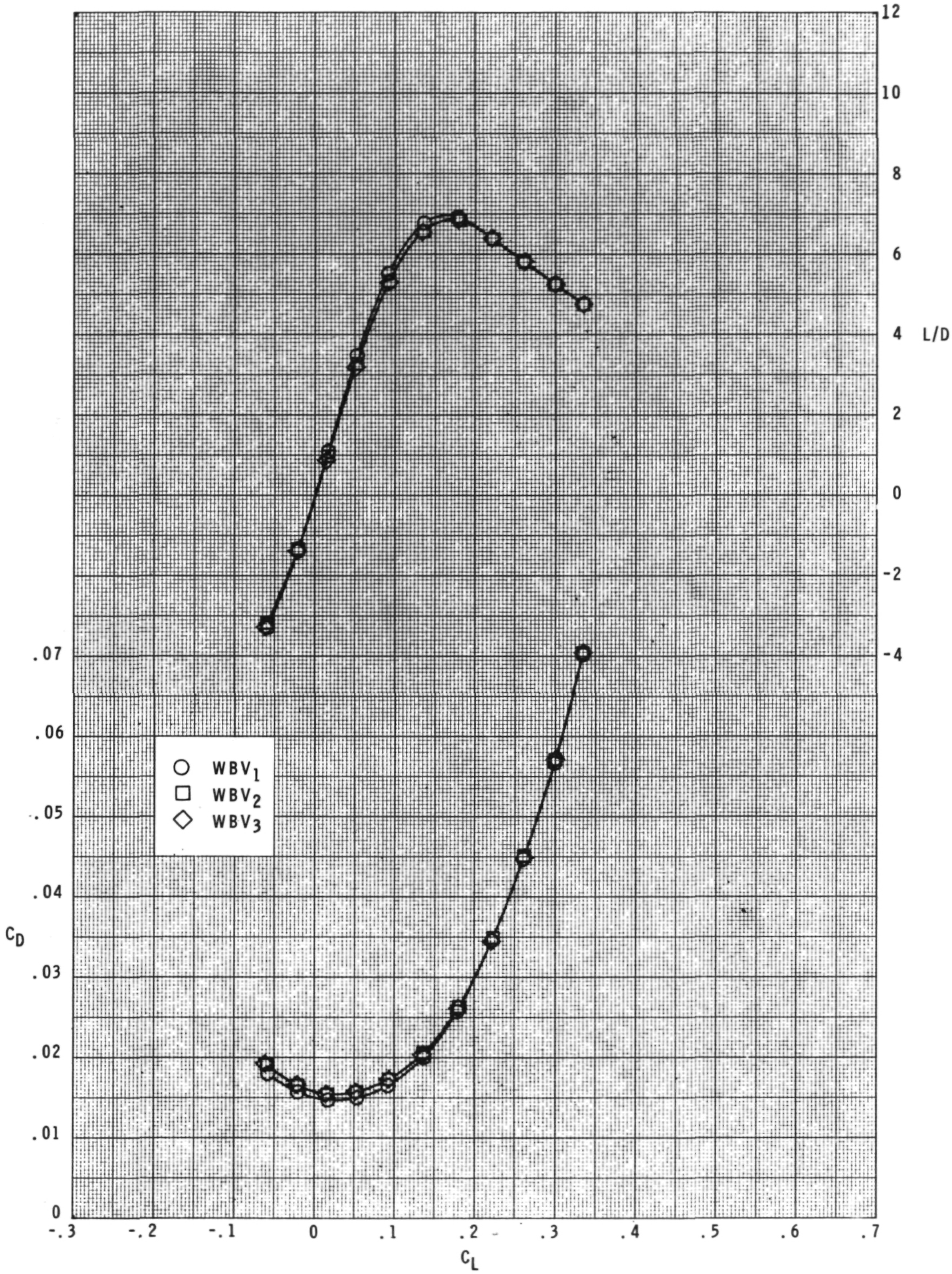

(b) M = 2.00, concluded.

Figure 5.- Continued.

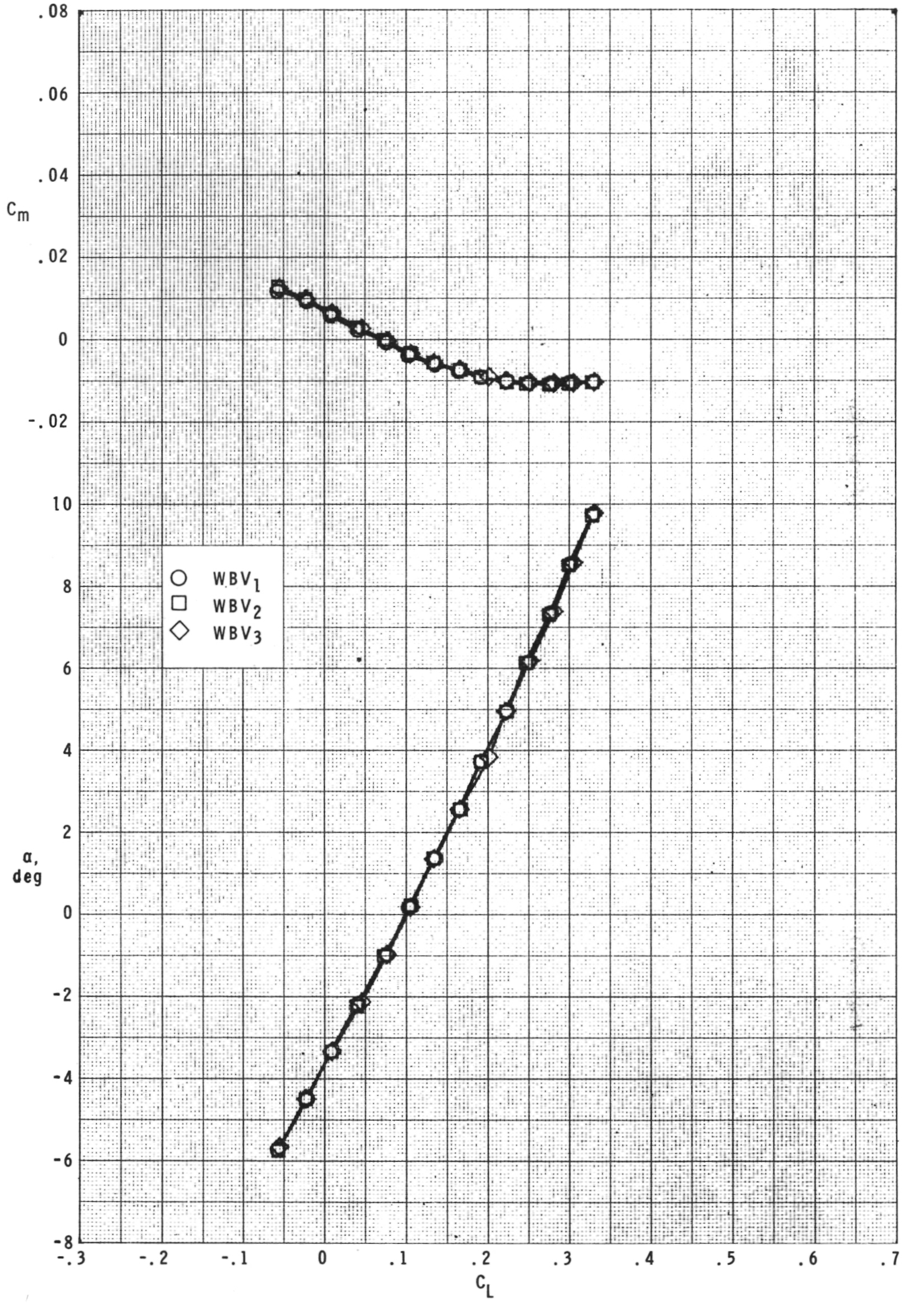

(c) M = 2.60.

Figure 5.- Continued.

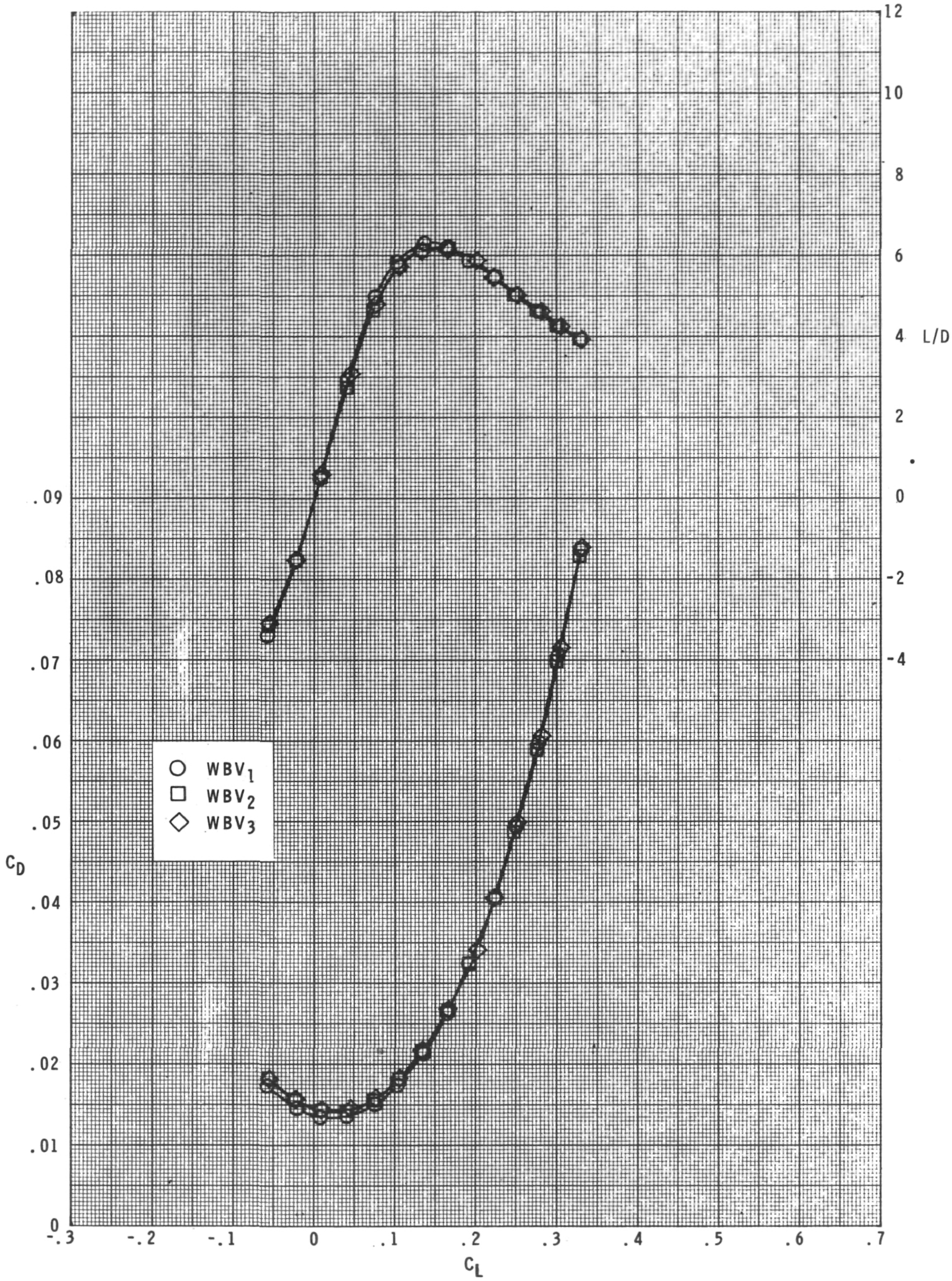

(c) M = 2.60, concluded.

Figure 5.- Concluded.

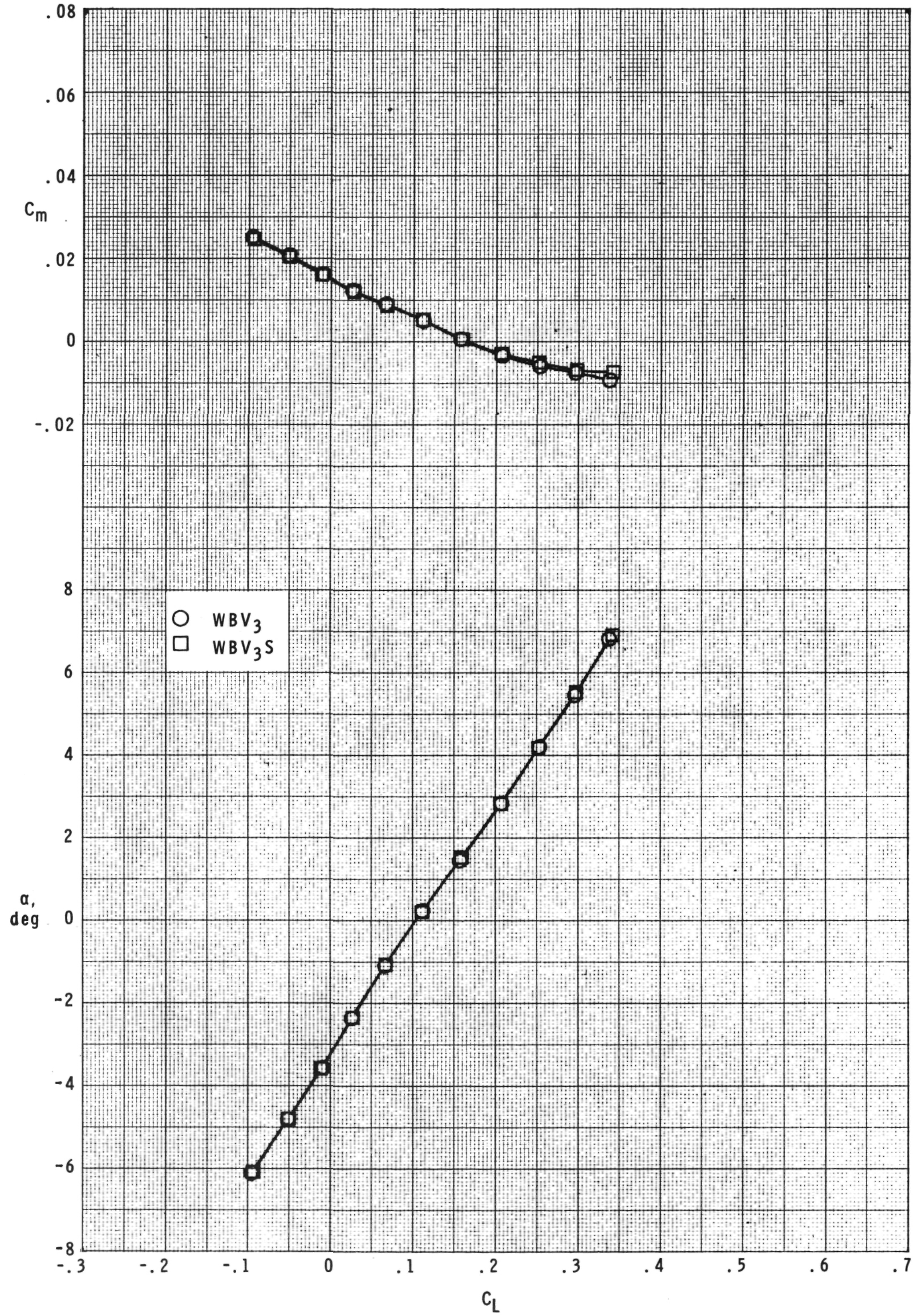

(a) M = 1.80.

Figure 6.- Effect of nose strakes on aerodynamic characteristics in pitch.

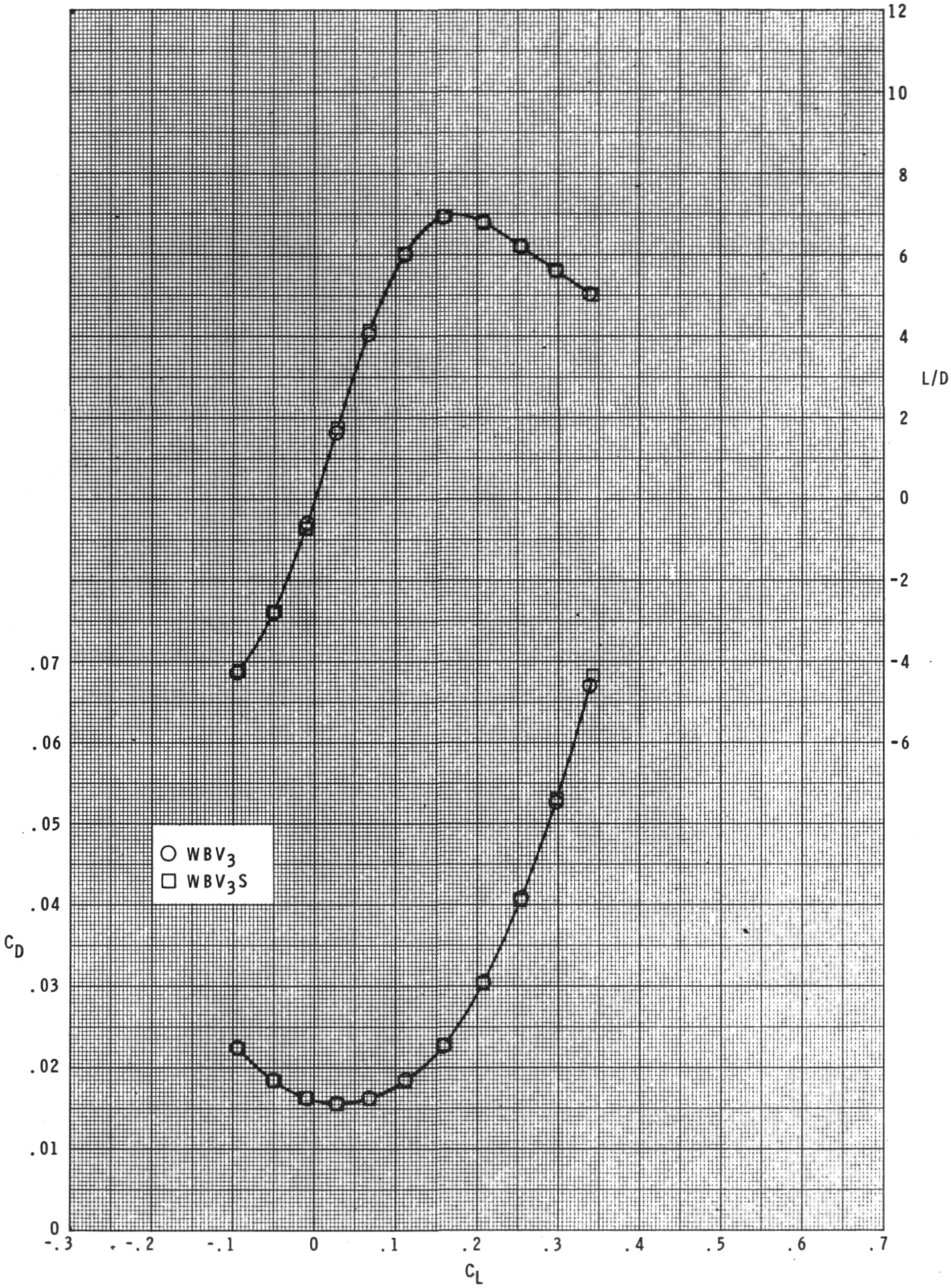

(a) M = 1.80, concluded.

Figure 6.- Continued.

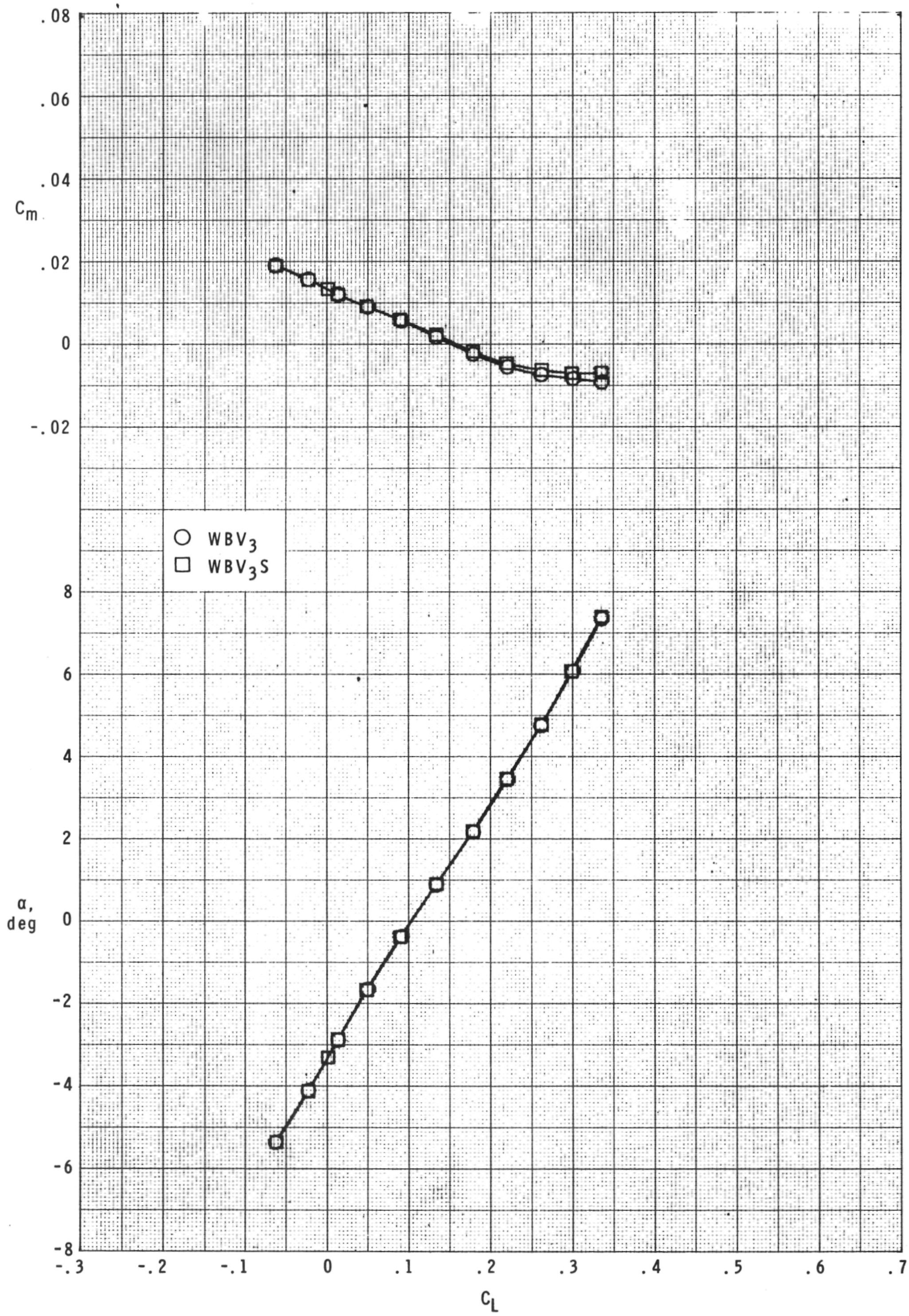

(b) M = 2.00.

Figure 6.- Continued.

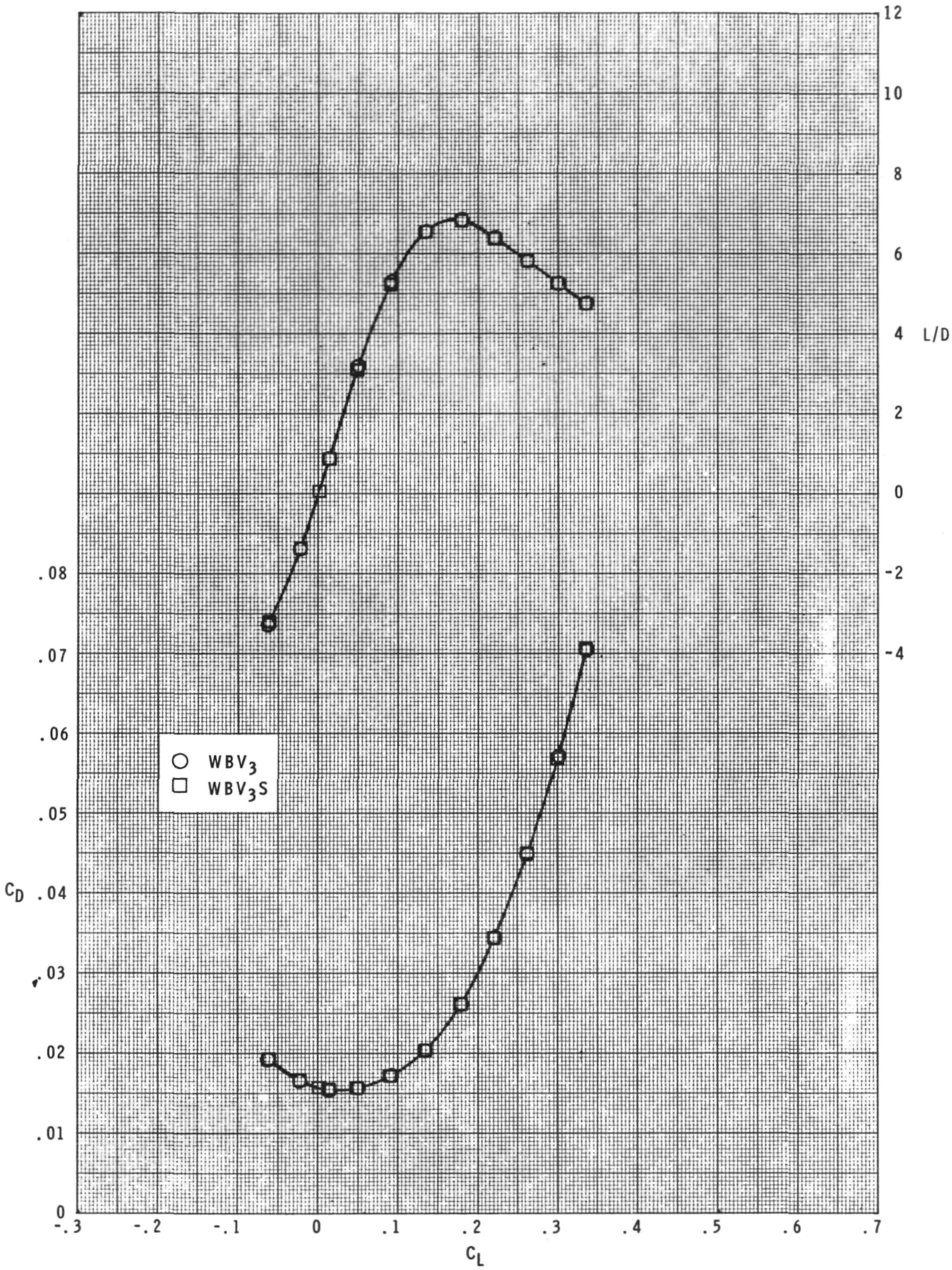

(b) M = 2.00, concluded.

Figure 6.- Continued.

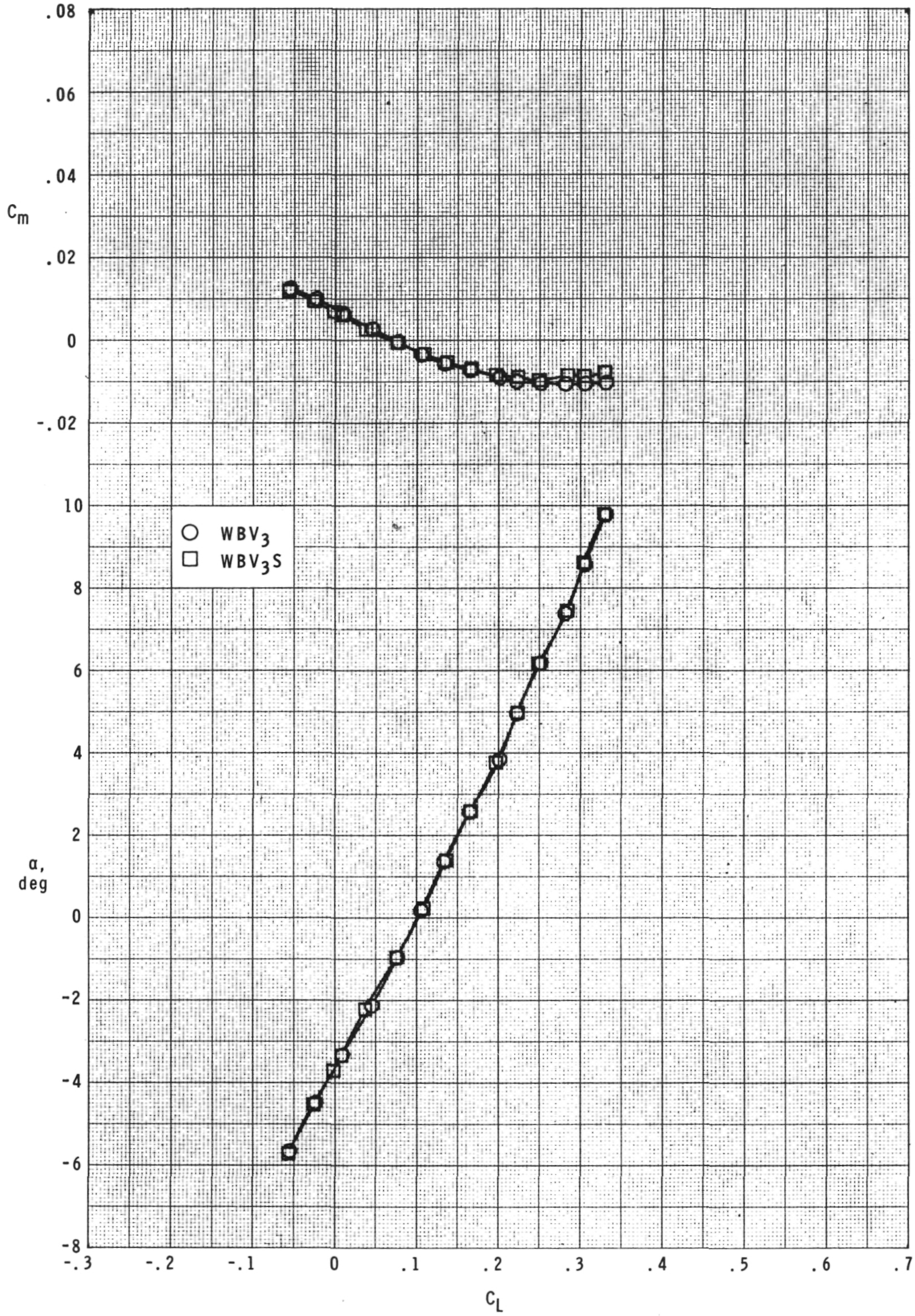

(c) M = 2.60.

Figure 6.- Continued.

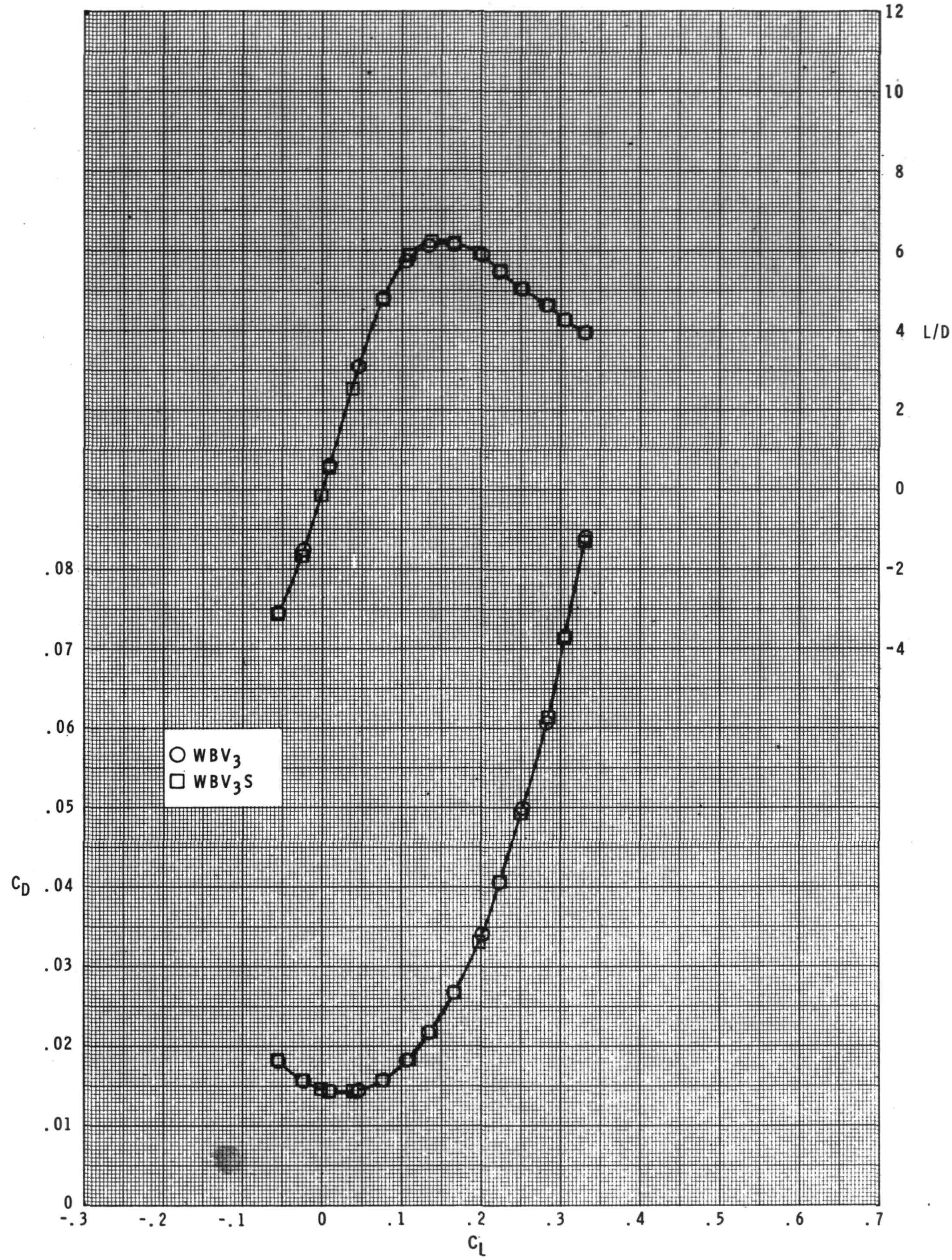

(c) M = 2.60, concluded.

Figure 6.- Concluded.

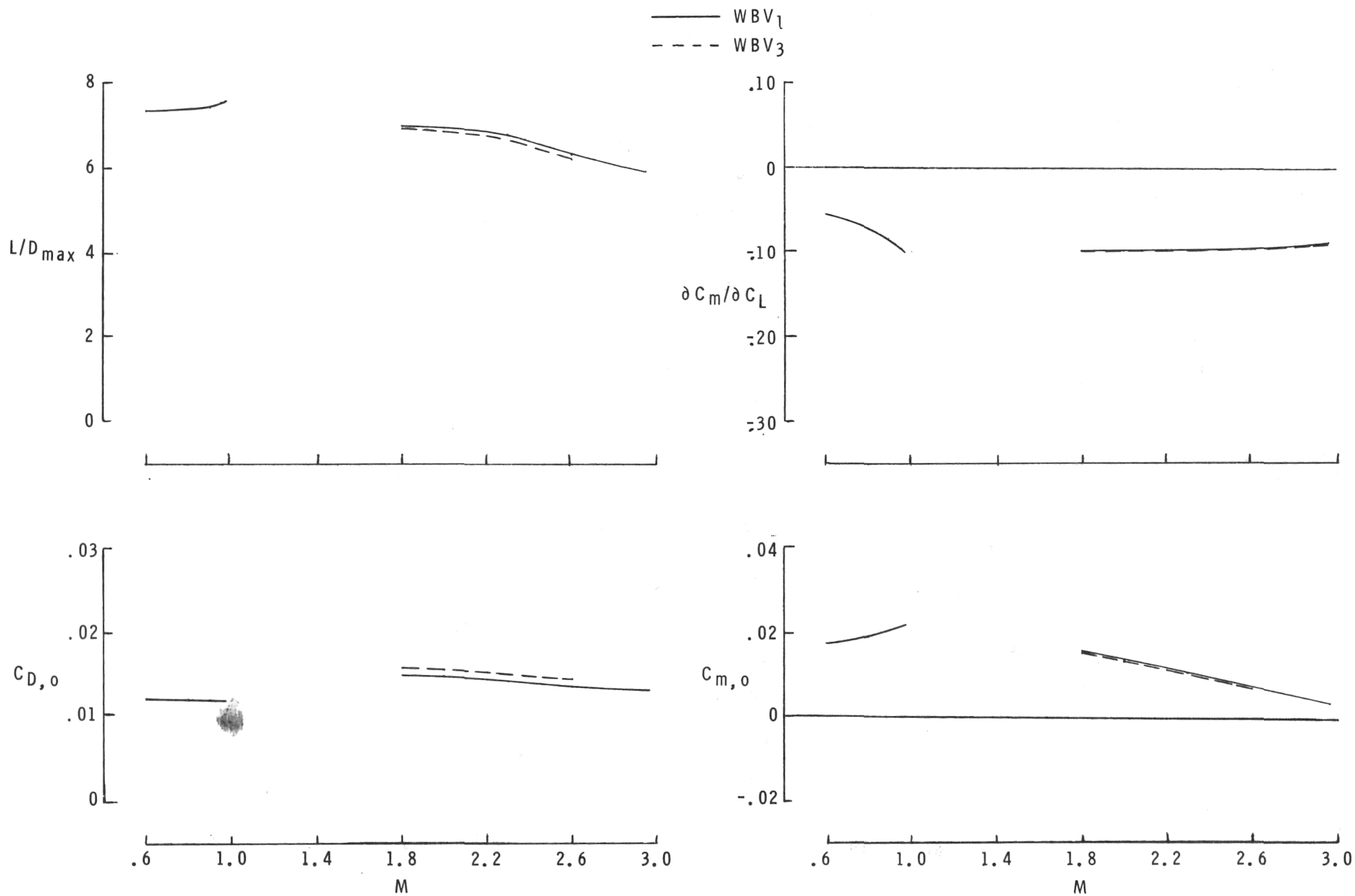

Figure 7.- Summary of longitudinal aerodynamic parameters.

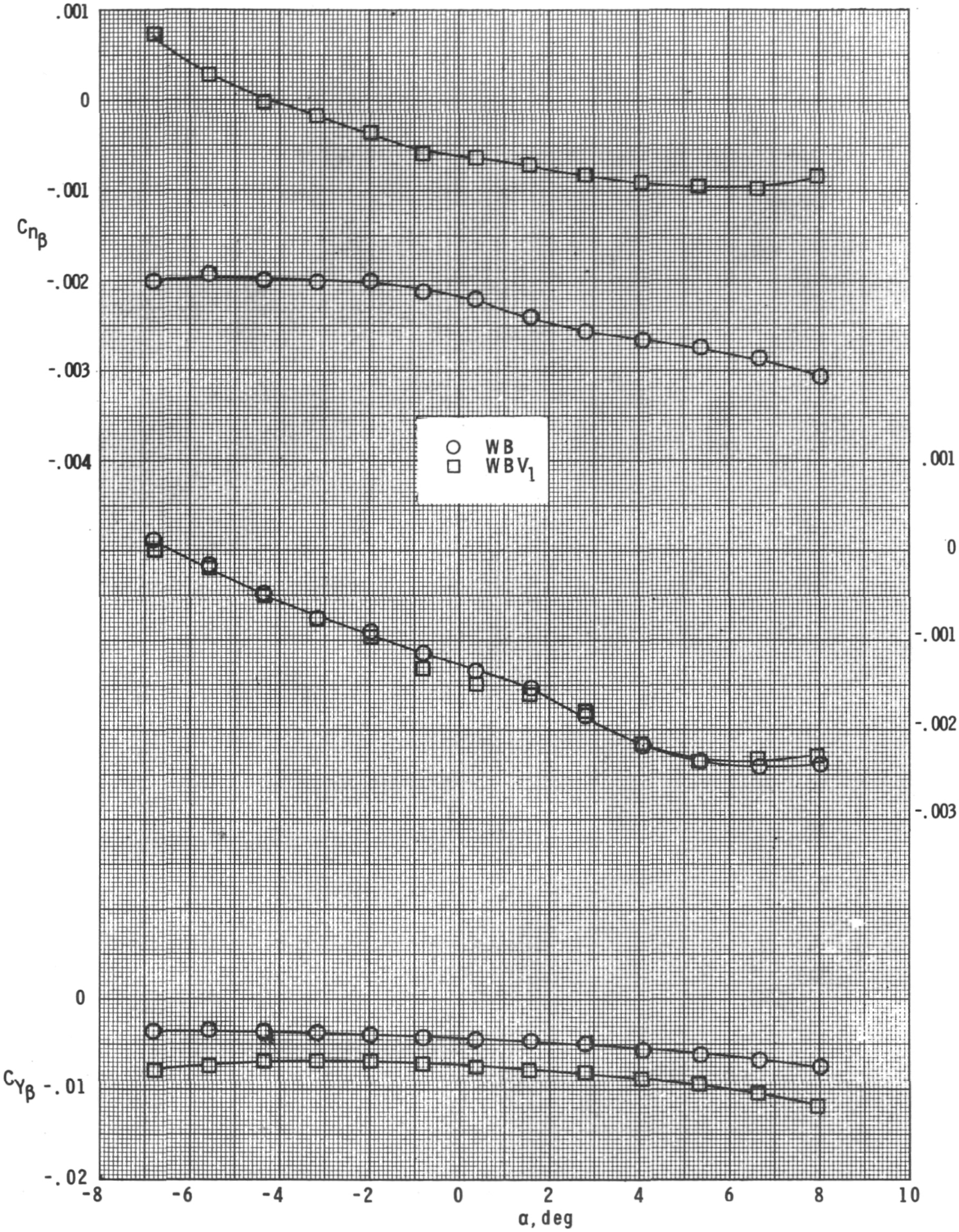

(a) M = 0.60.

Figure 8.- Comparison of lateral aerodynamic characteristics for complete basic model configuration with and without small vertical and ventral tails.

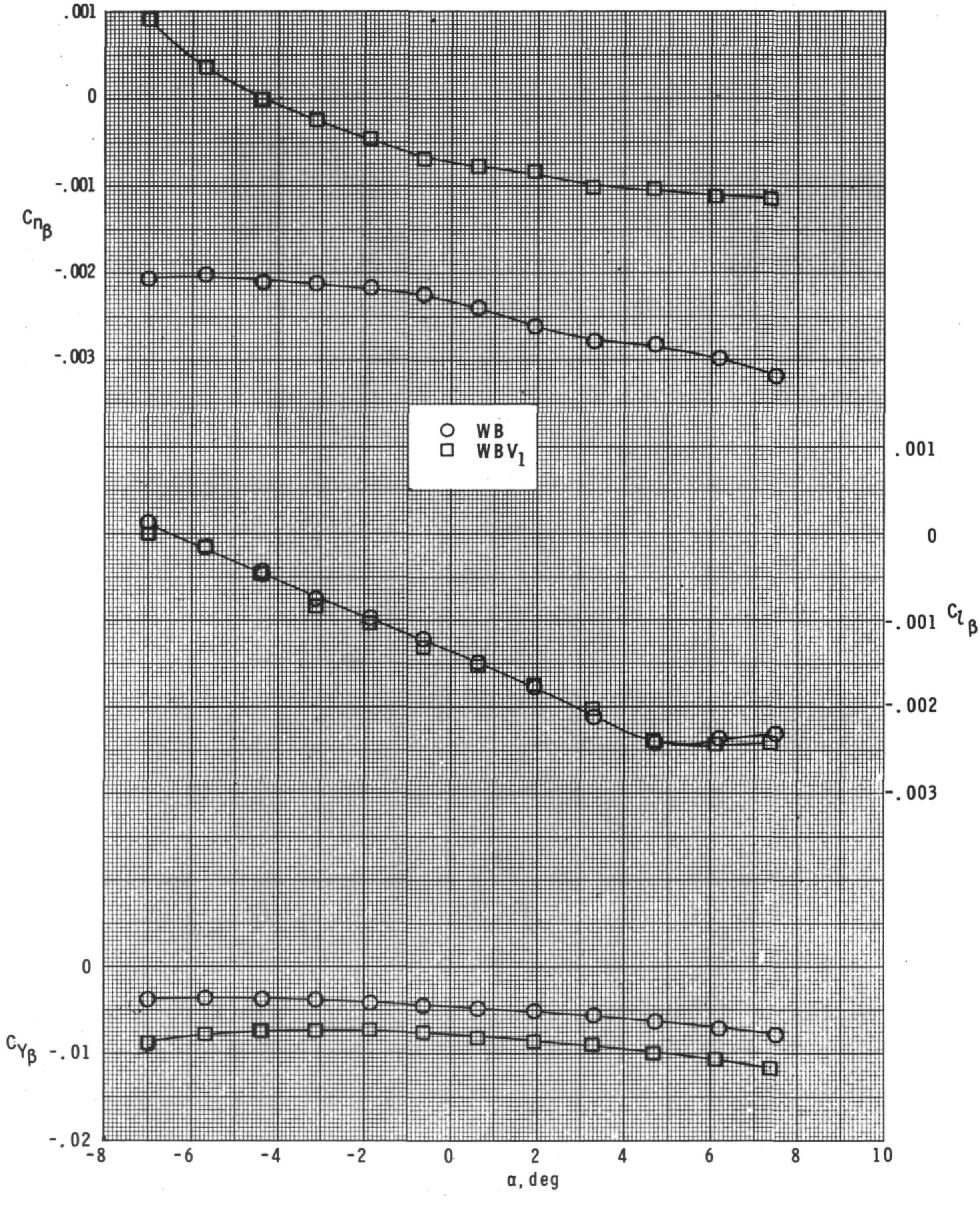

(b) M = 0.90.

Figure 8.- Continued.

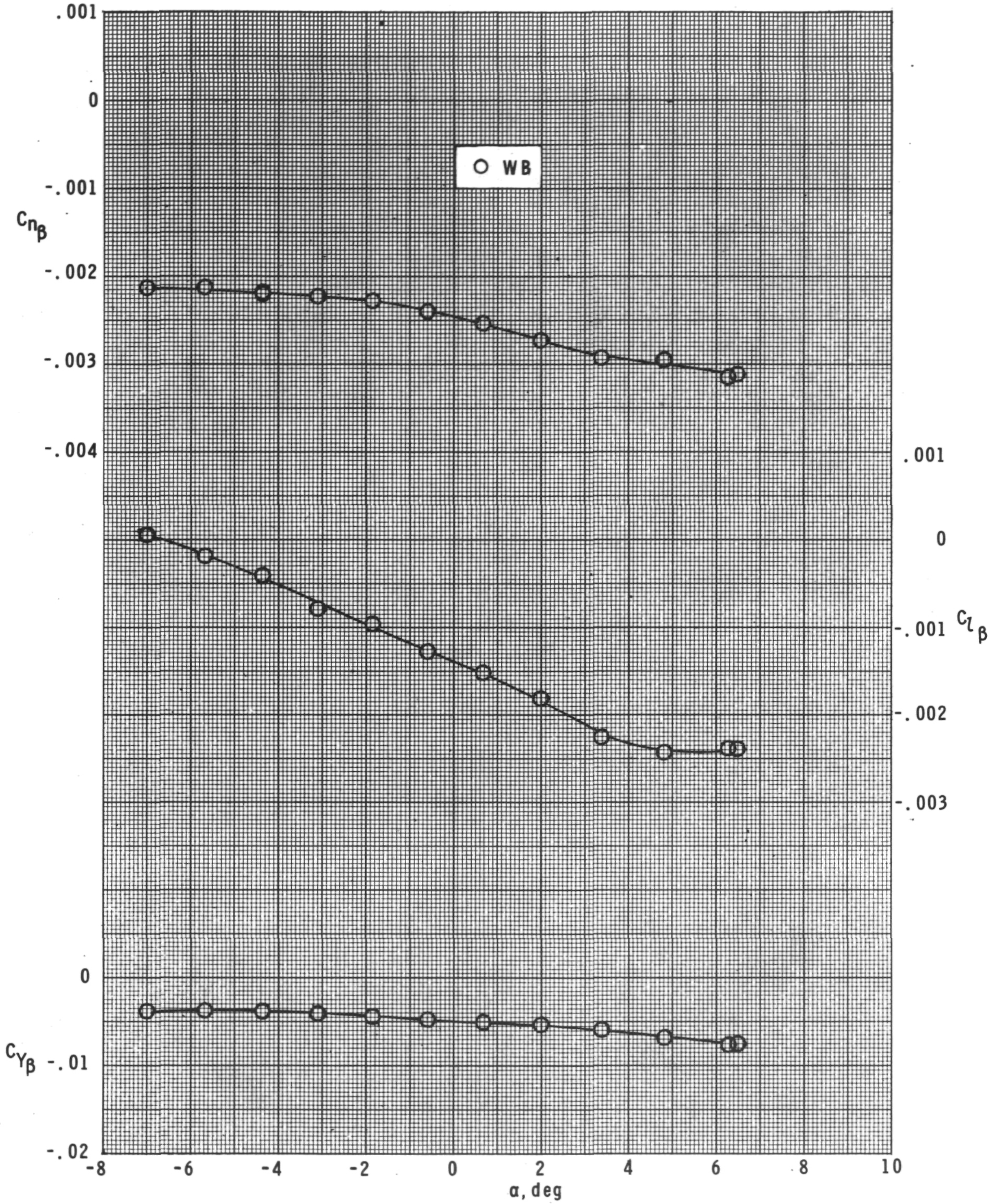

(c) M = 0.97.

Figure 8.- Continued.

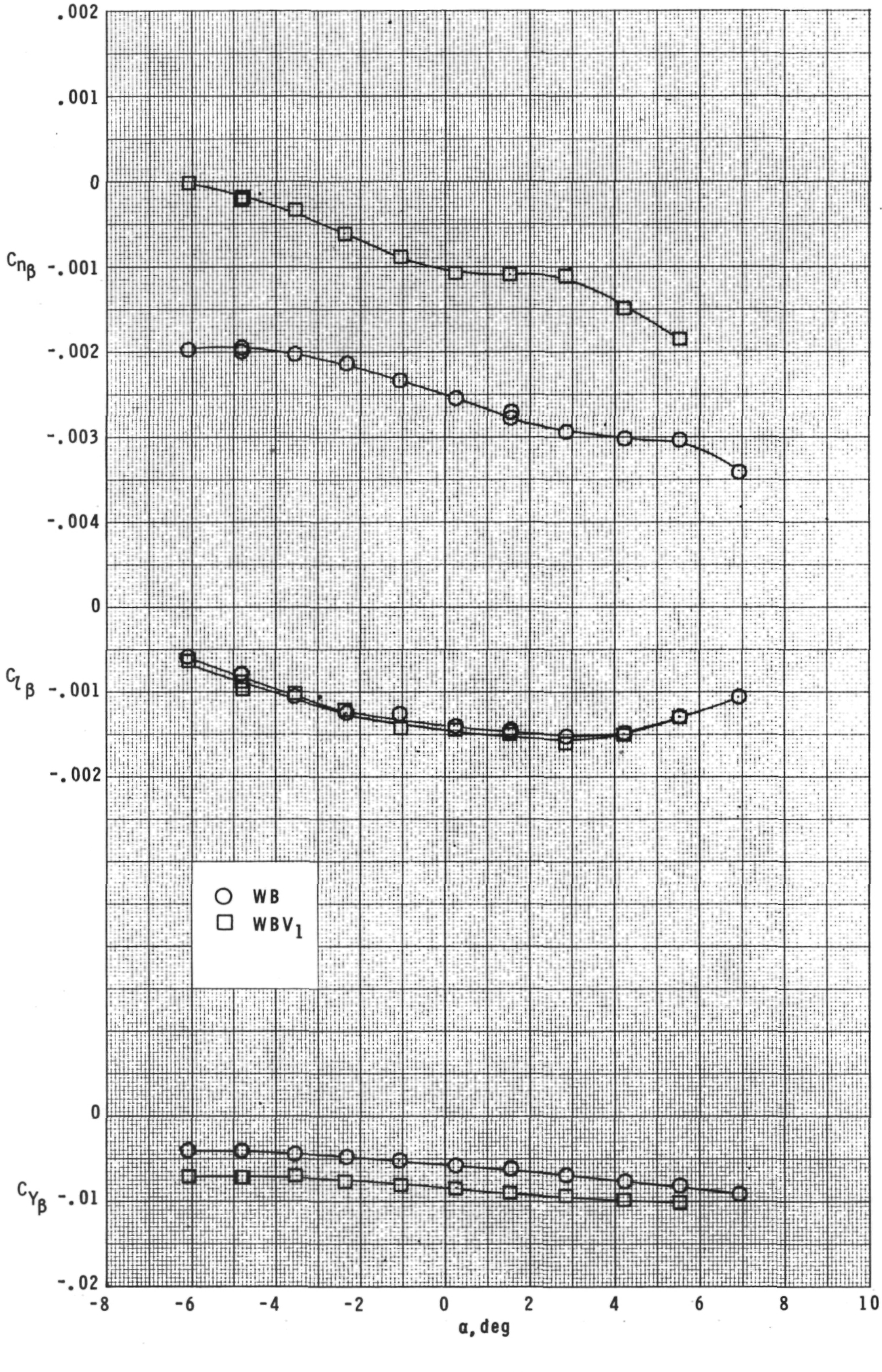

(d) M = 1.80.

Figure 8.- Continued.

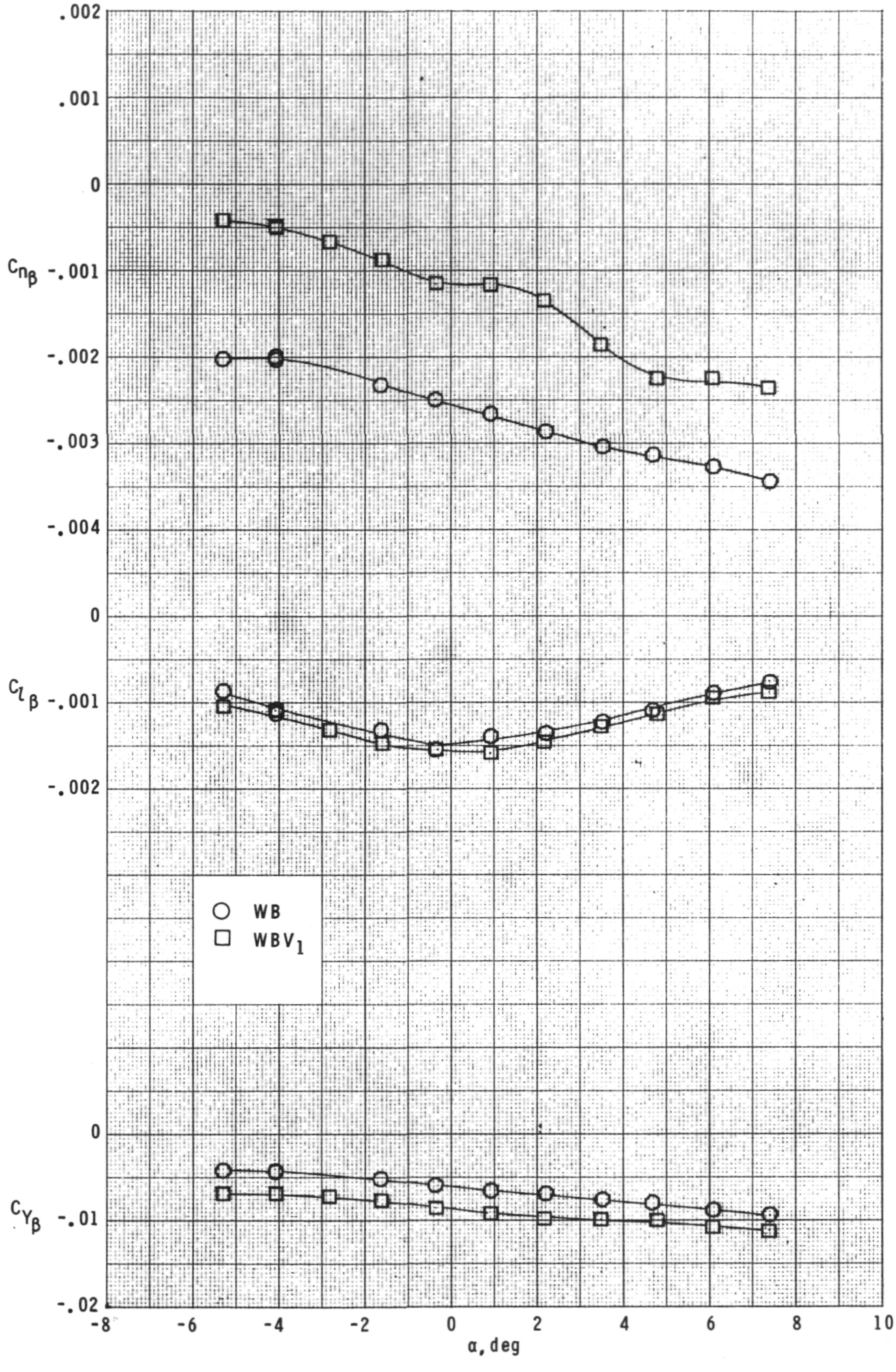

(e) M = 2.00.

Figure 8.- Continued.

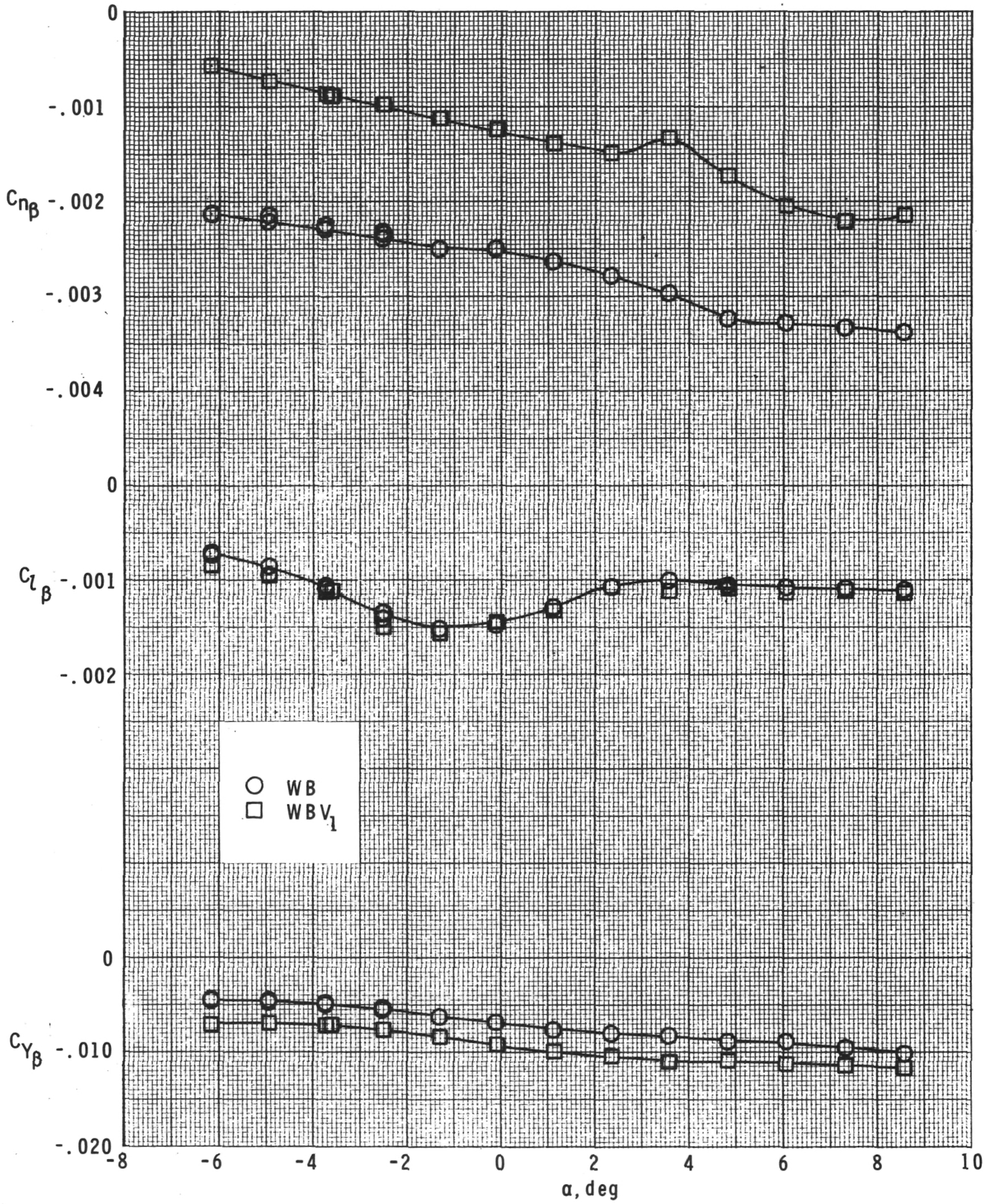

(f) M = 2.30.

Figure 8.- Continued.

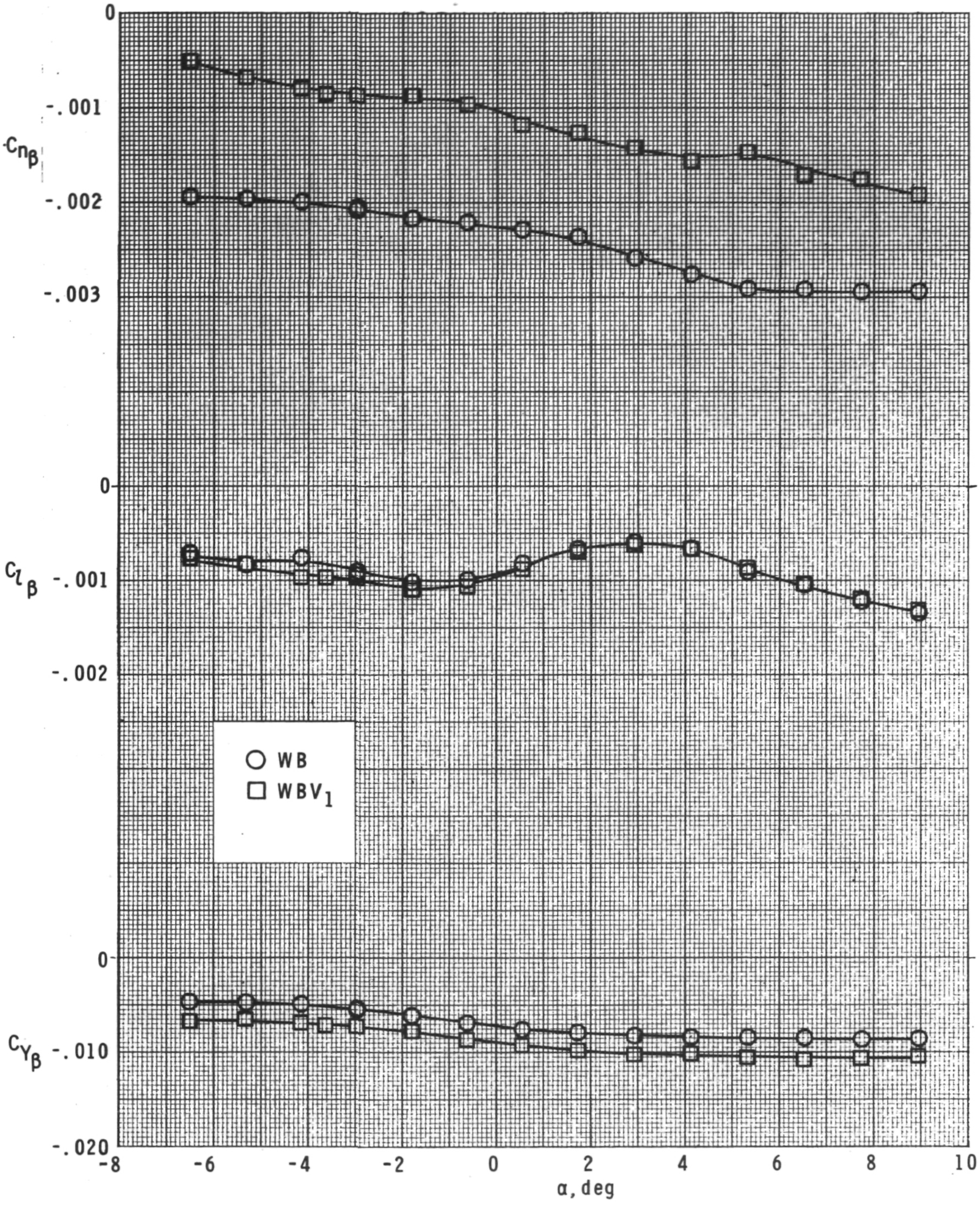

(g) M = 2.60.

Figure 8.- Continued.

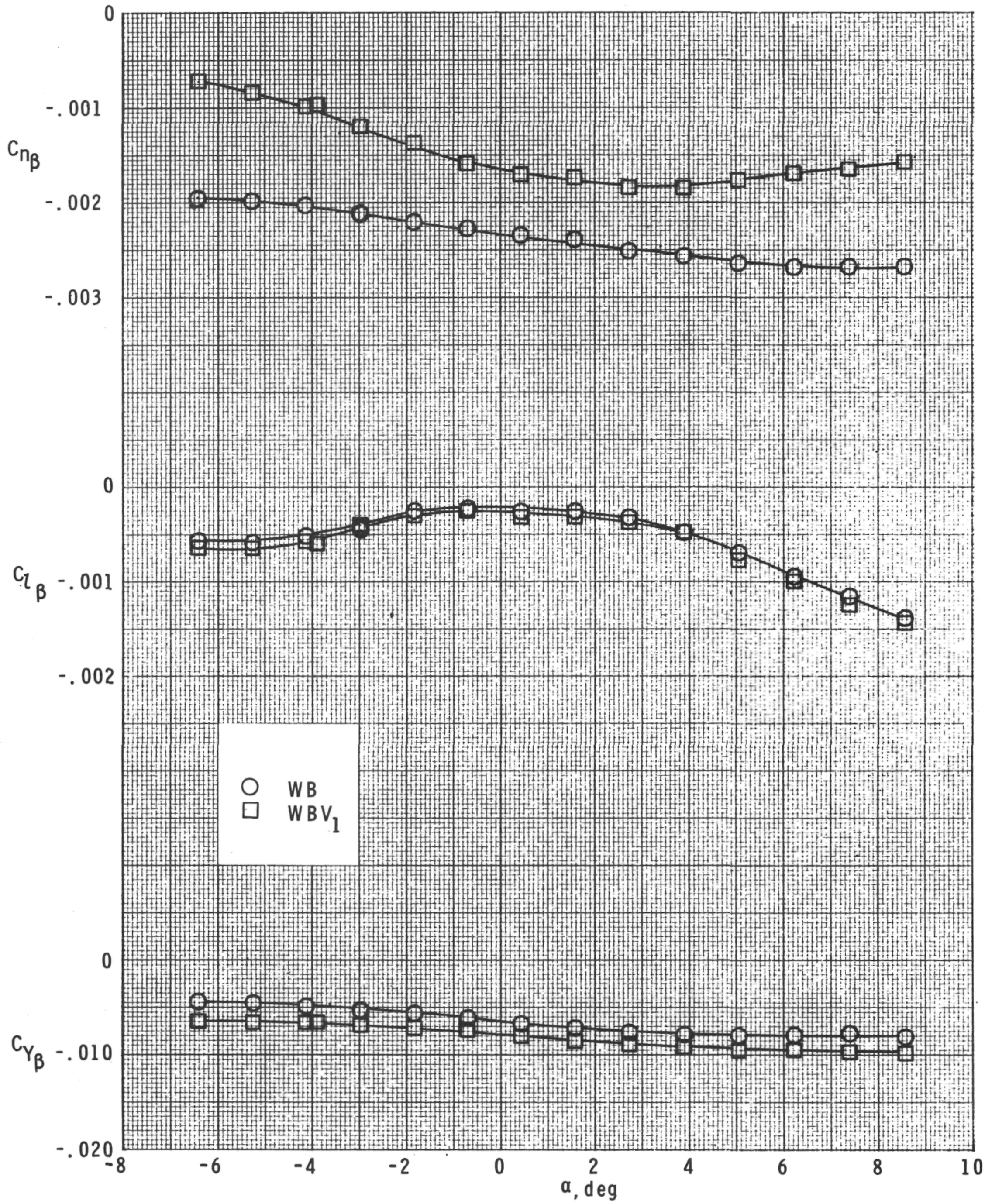

(h) M = 2.96.

Figure 8.- Concluded.

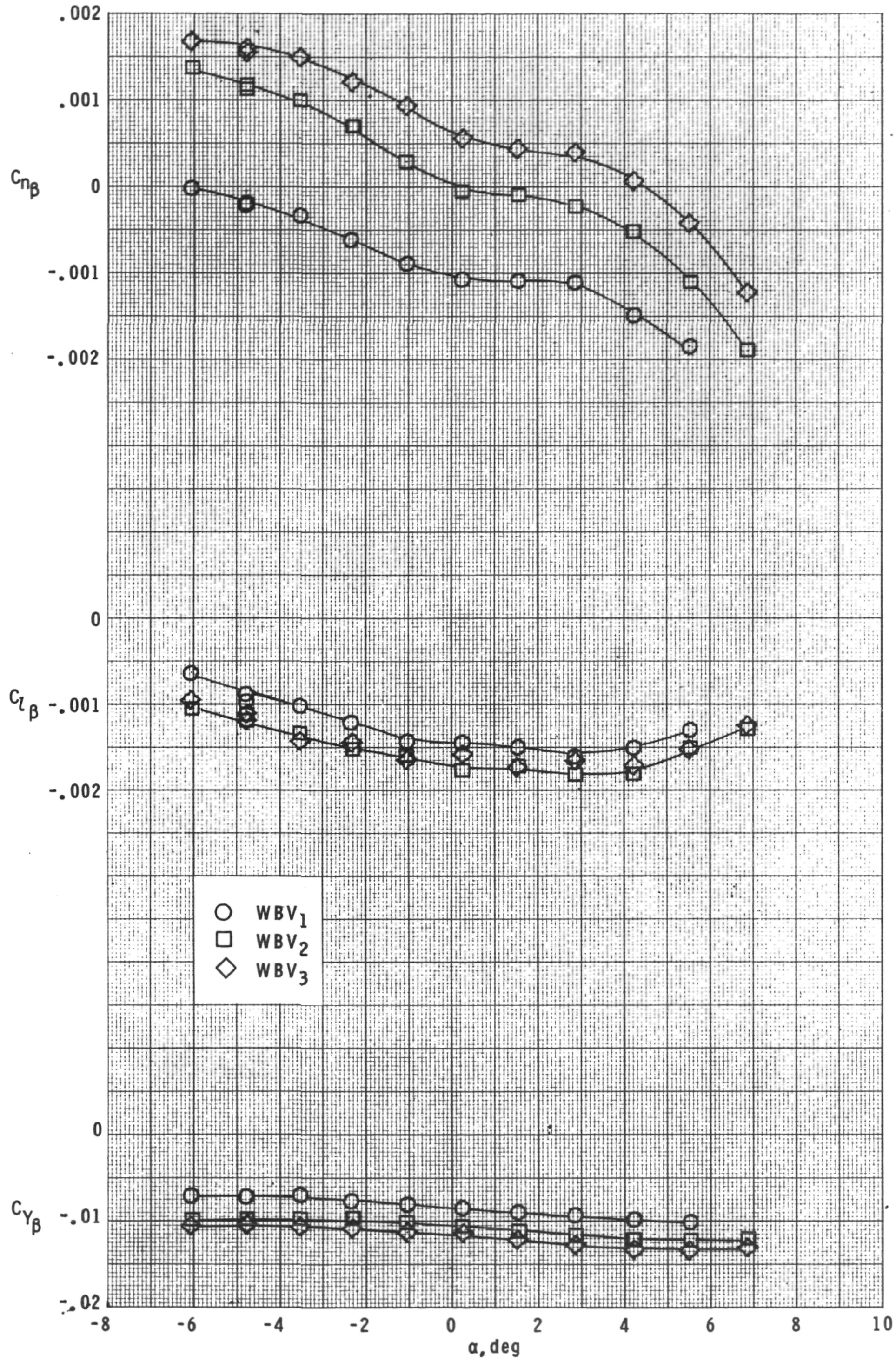

(a) M = 1.80.

Figure 9.- Effect of vertical and ventral tail size on lateral aerodynamic characteristics.

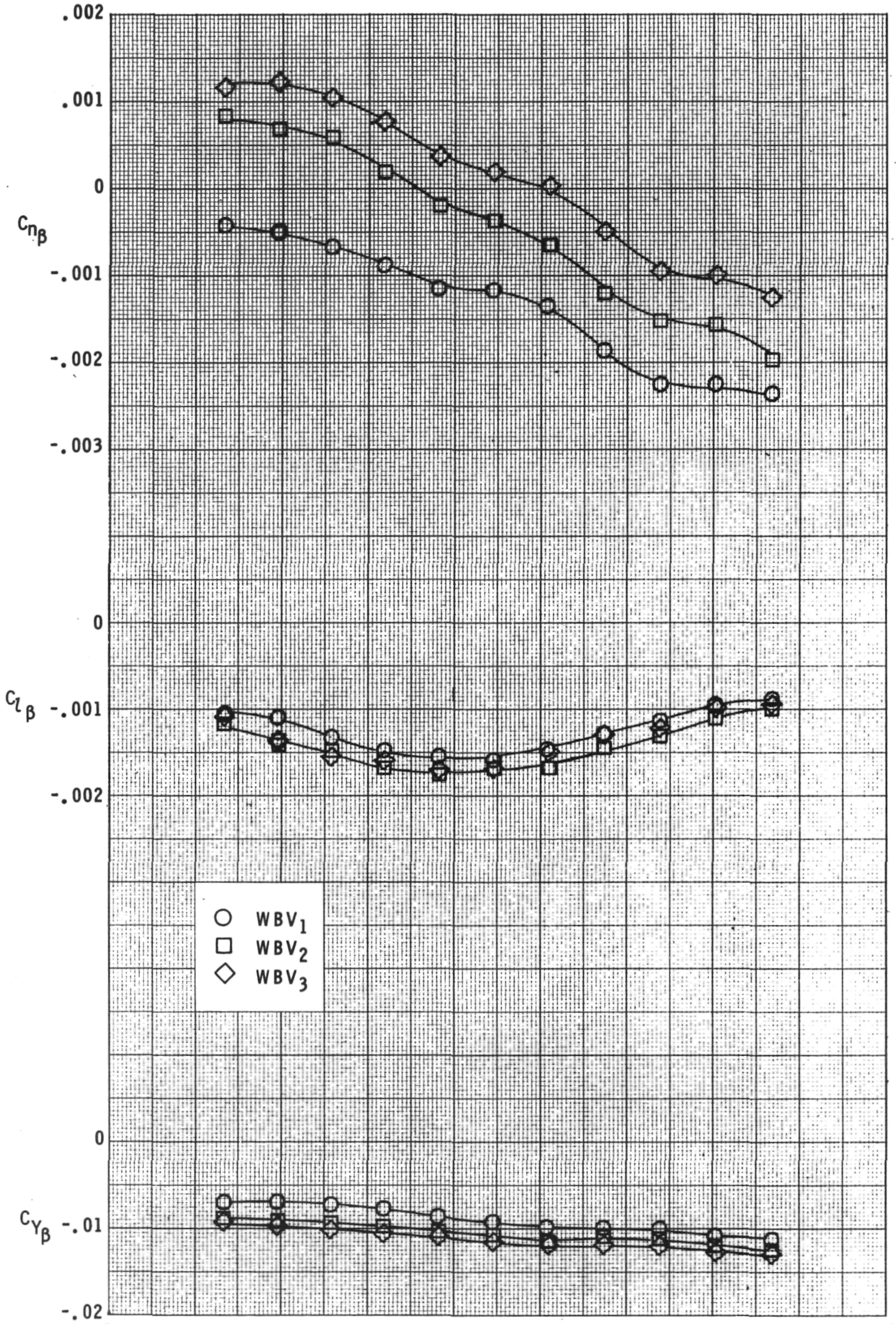

(b) M = 2.00.

Figure 9.- Continued.

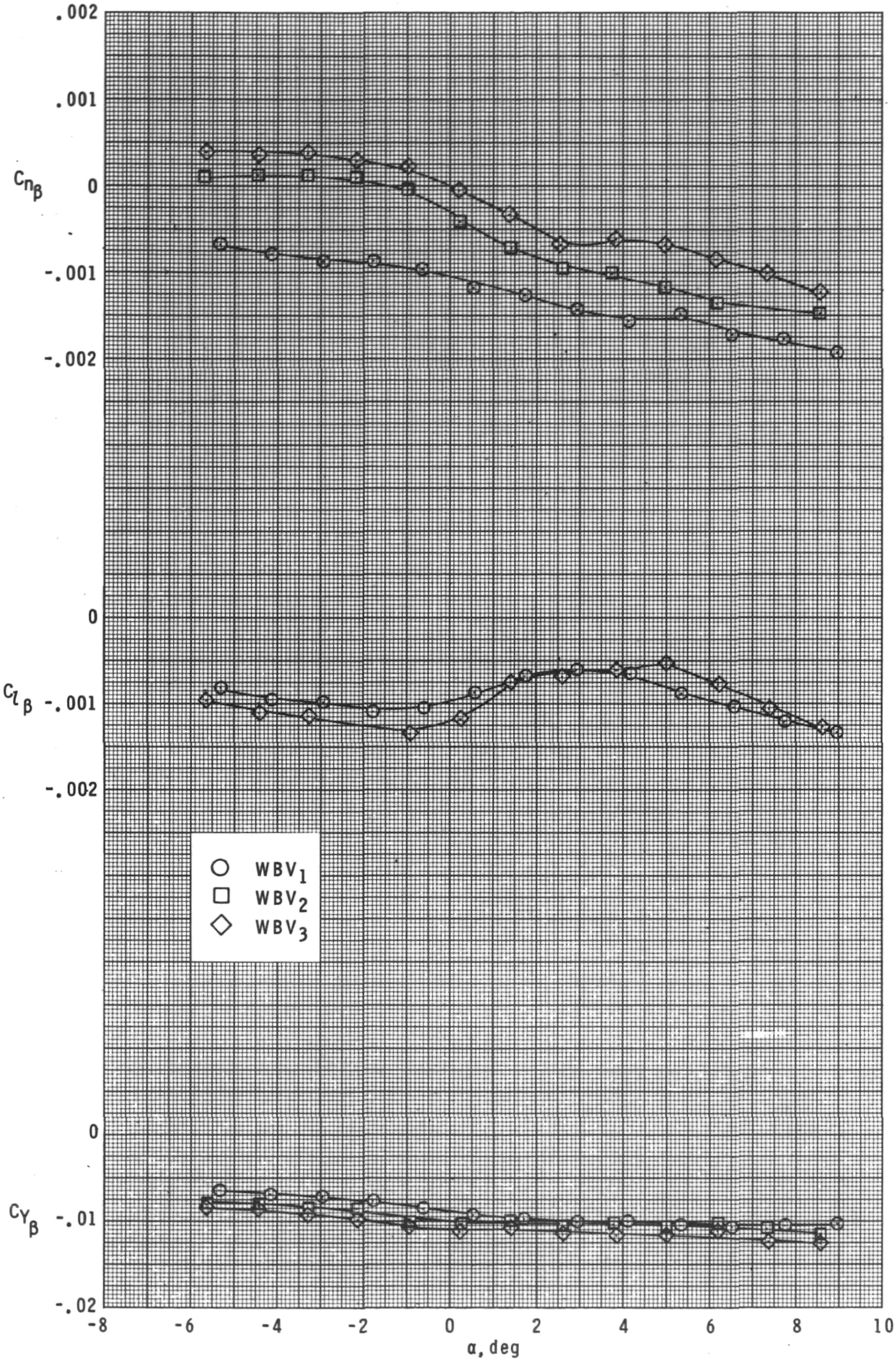

(c) M = 2.60.

Figure 9.- Concluded.

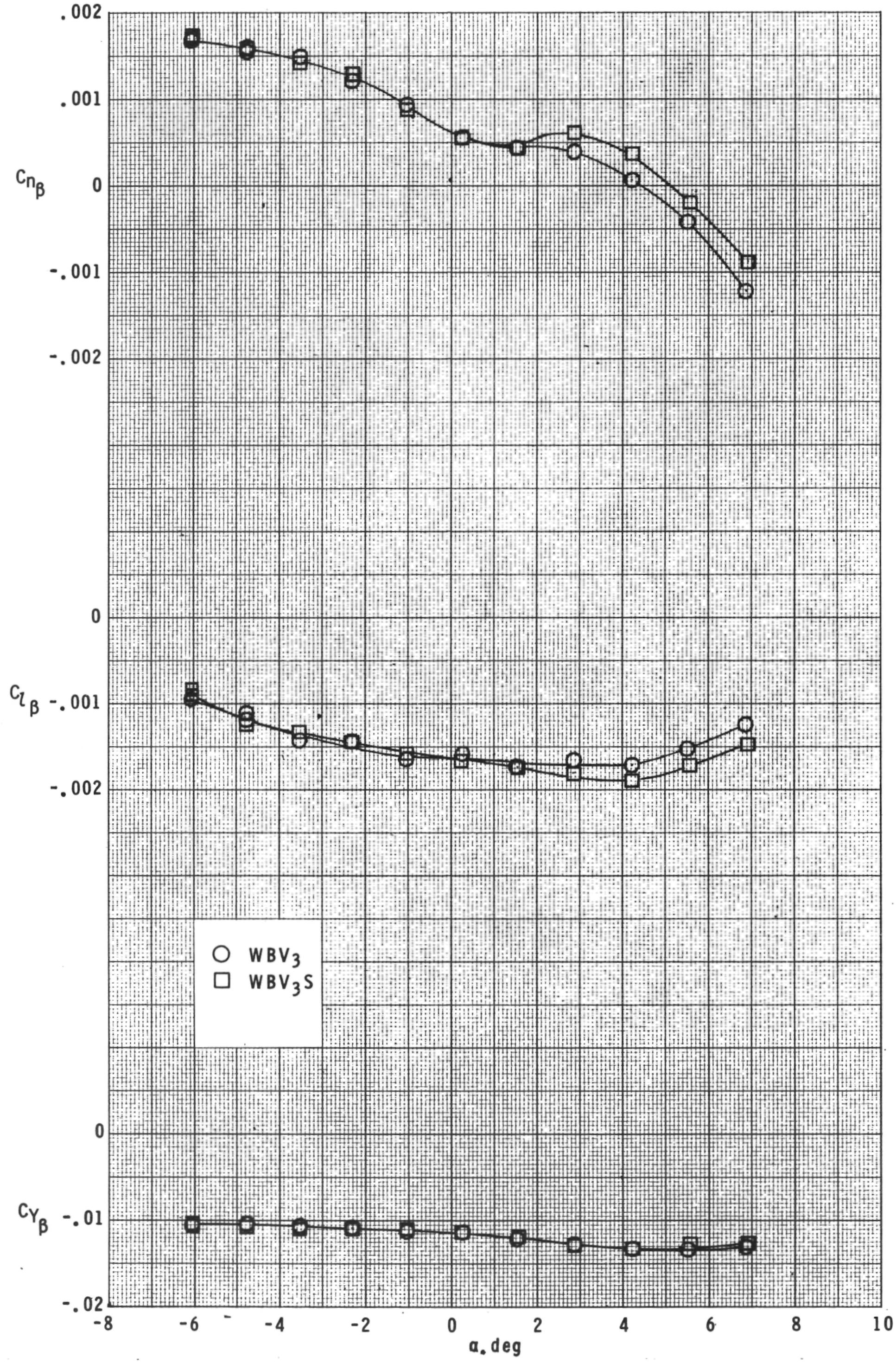

(a) M = 1.80.

Figure 10.- Effect of fuselage nose strakes on lateral aerodynamic characteristics.

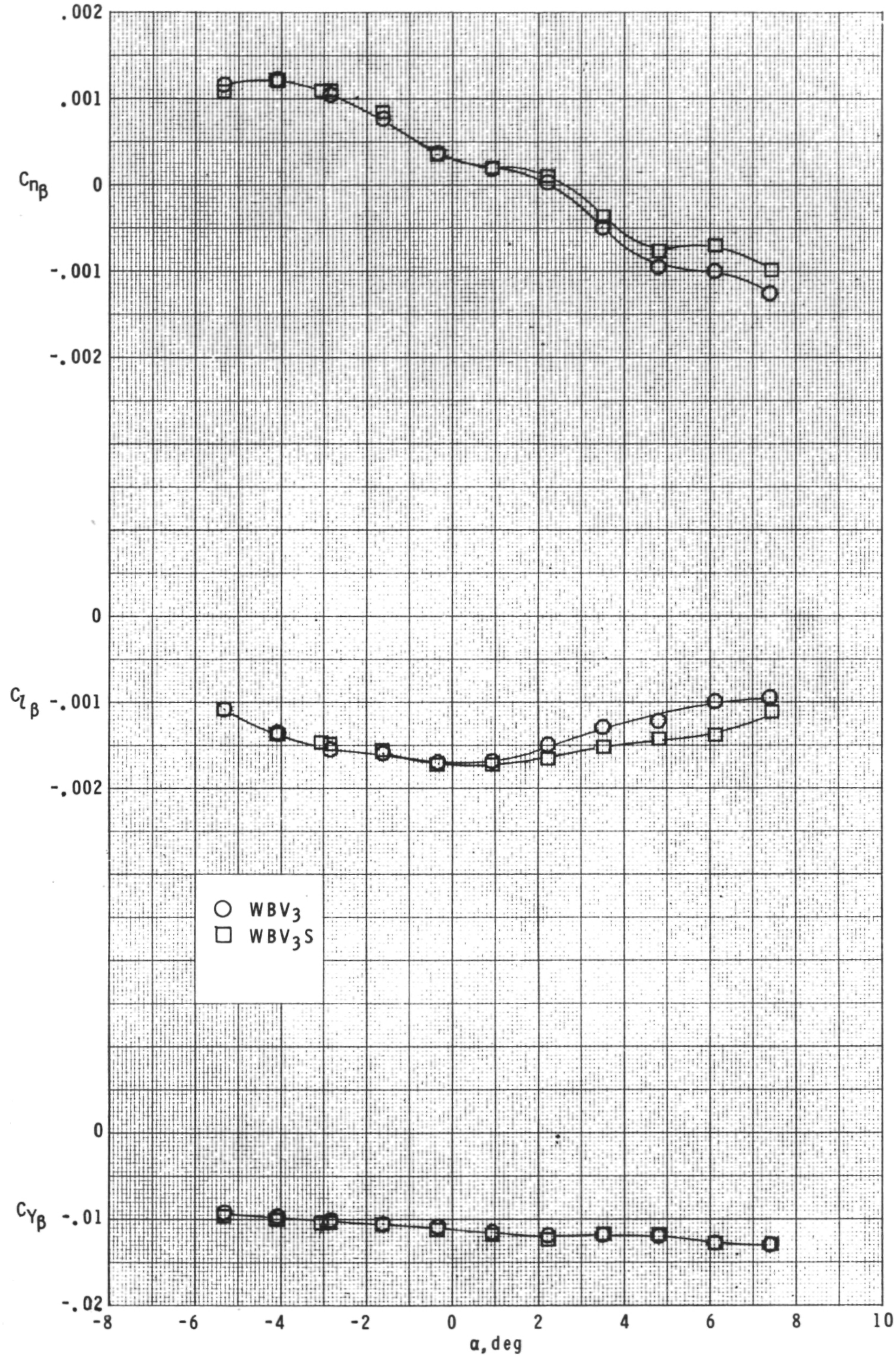

(b) M = 2.00.

Figure 10.- Continued.

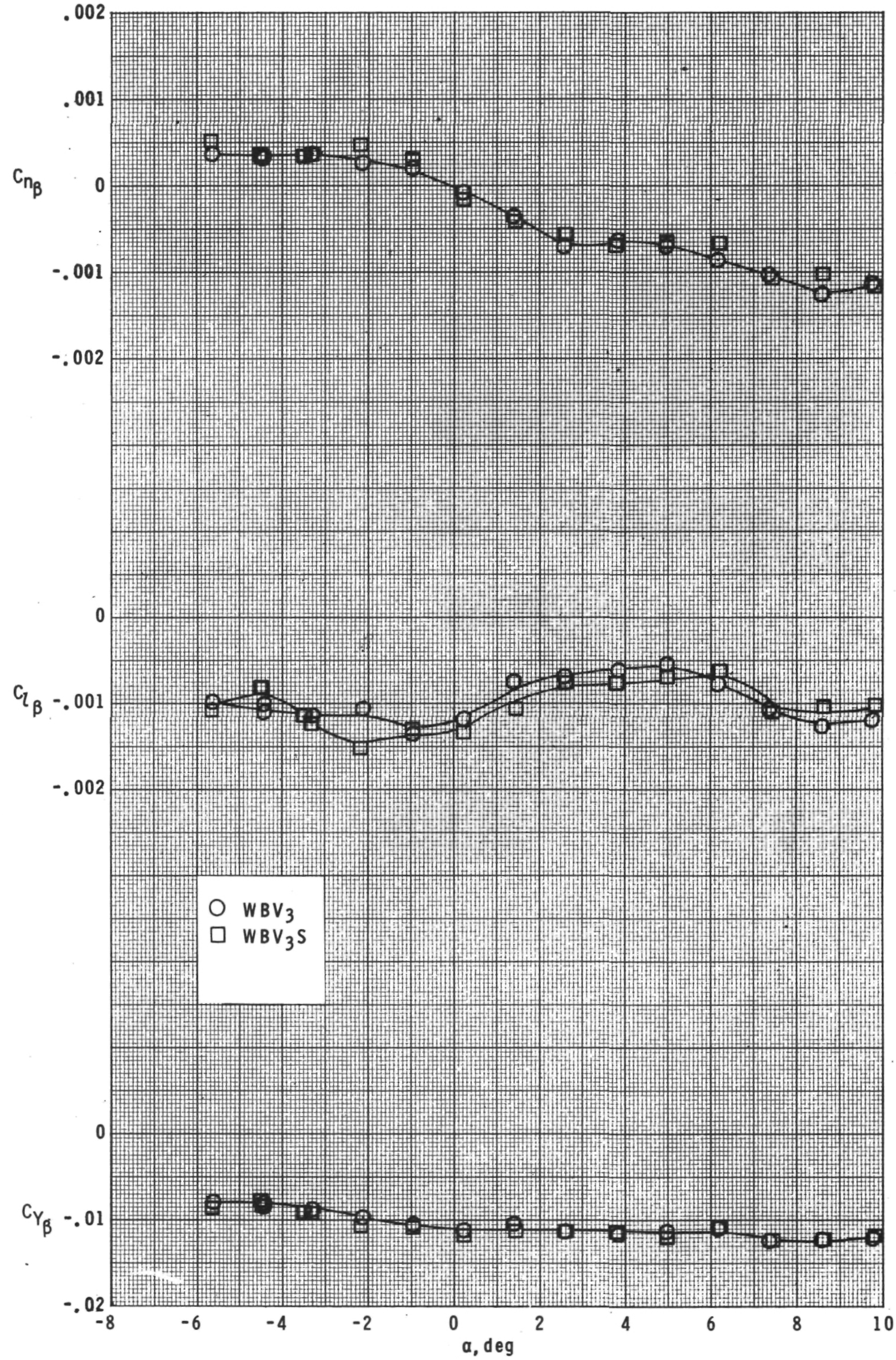

(c) M = 2.60.

Figure 10.- Concluded.

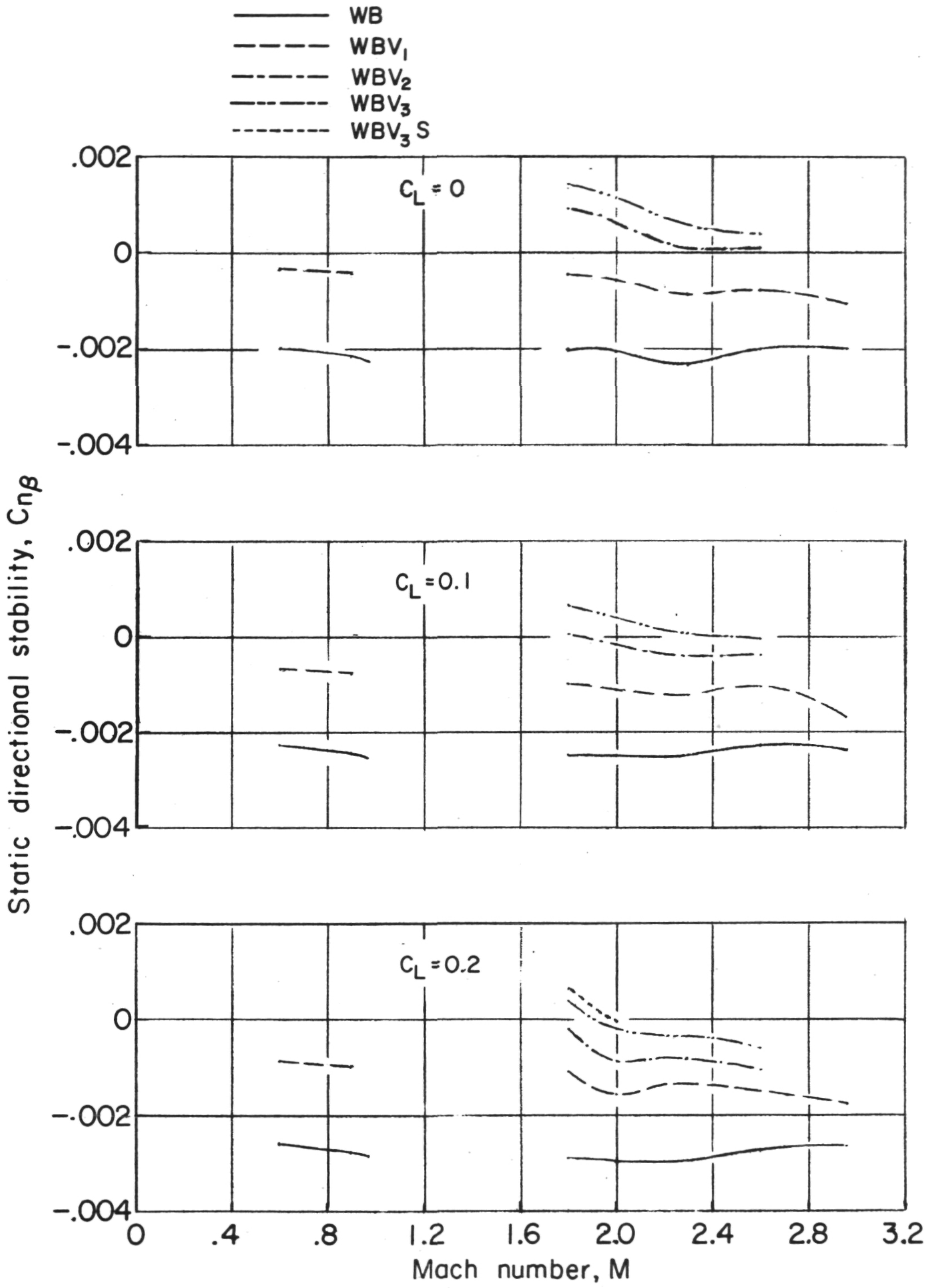

Figure 11.- Summary of static directional stability characteristics at various lift coefficients with and without various vertical tails and nose strakes.

"The aeronautical and space activities of the United States shall be conducted so as to contribute . . . to the expansion of human knowledge of phenomena in the atmosphere and space. The Administration shall provide for the widest practicable and appropriate dissemination of information concerning its activities and the results thereof."

—NATIONAL AERONAUTICS AND SPACE ACT OF 1958

NASA SCIENTIFIC AND TECHNICAL PUBLICATIONS

TECHNICAL REPORTS: Scientific and technical information considered important, complete, and a lasting contribution to existing knowledge.

TECHNICAL NOTES: Information less broad in scope but nevertheless of importance as a contribution to existing knowledge.

TECHNICAL MEMORANDUMS: Information receiving limited distribution because of preliminary data, security classification, or other reasons. Also includes conference proceedings with either limited or unlimited distribution.

CONTRACTOR REPORTS: Scientific and technical information generated under a NASA contract or grant and considered an important contribution to existing knowledge.

TECHNICAL TRANSLATIONS: Information published in a foreign language considered to merit NASA distribution in English.

SPECIAL PUBLICATIONS: Information derived from or of value to NASA activities. Publications include final reports of major projects, monographs, data compilations, handbooks, sourcebooks, and special bibliographies.

TECHNOLOGY UTILIZATION PUBLICATIONS: Information on technology used by NASA that may be of particular interest in commercial and other non-aerospace applications. Publications include Tech Briefs, Technology Utilization Reports and Technology Surveys.

Details on the availability of these publications may be obtained from:

SCIENTIFIC AND TECHNICAL INFORMATION OFFICE

NATIONAL AERONAUTICS AND SPACE ADMINISTRATION

Washington, D.C. 20546